

1    **The gut microbiota is essential for *Trichinella spiralis*- evoked  
2    suppression of colitis**

3    **Short title:** Gut microbiota mediate *T. spiralis*- evoked suppression of colitis

4

5    Hualei Sun<sup>1#\*</sup>, Shao Rong Long<sup>2#</sup>, Miao Jiang<sup>2#</sup>, Hui Ran Zhang<sup>2</sup>, Jing Jing Wang<sup>2</sup>, Zi  
6    Xuan Liao<sup>2</sup>, Jing Cui<sup>2</sup>, Zhong Quan Wang<sup>2</sup>

7

8    <sup>1</sup>Department of Nutrition, the First Affiliated Hospital of Zhengzhou University,  
9    Zhengzhou, Henan, 450052, China

10    <sup>2</sup>Department of Pathogen Biology, Medical College of Zhengzhou University,  
11    Zhengzhou, Henan, 450001, China

12    <sup>#</sup>These authors contributed equally: Hualei Sun, Shao Rong Long and Miao Jiang

13    \*Corresponding authors: Correspondence should be addressed to Hualei Sun  
14    (sunhualei911@foxmail.com)

15

16

17

18

19

20

21

22

23 **Abstract**

24 Inflammatory bowel disease (IBD) increases the risk of colorectal cancer, and it has  
25 the potential to diminish the quality of life. Clinical and experimental evidence  
26 demonstrate protective aspects of parasitic helminth infection against IBD. However,  
27 studies on the inhibition of inflammation by helminth infection have overlooked a key  
28 determinant of health: the gut microbiota. Infection with helminths induces alterations  
29 in the host microbiota composition. However, the potential influence and mechanism  
30 of helminth infections induced changes in the gut microbiota on the development of  
31 IBD has not yet been elucidated. In this study, we analyzed the intersection of  
32 helminth *Trichinella spiralis* and gut bacteria in the regulation of colitis and related  
33 mechanisms. *T. spiralis* infected mice were treated with antibiotics or cohoused with  
34 wild type mice, then challenged with DSS-colitis and disease severity, immune  
35 responses and goblet cells assessed. Gut bacteria composition was assessed by 16 s  
36 rRNA sequencing and SCFAs were measured. Results showed that protection against  
37 disease by infection with *T. spiralis* was abrogated by antibiotic treatment, and  
38 cohousing with *T. spiralis*- infected mice suppressed DSS-colitis in wild type mice.  
39 Bacterial community profiling revealed an increase in the abundance of the bacterial  
40 genus *Muribaculum* and *unclassified\_Muribaculaceae* in mice with *T. spiralis*  
41 infection or mice cohoused with *T. spiralis*- infected mice. Metabolomic analysis  
42 demonstrated increased propionic acid in feces from *T. spiralis*- infected mice. Data  
43 also showed that the gut microbiome modulated by *T. spiralis* exhibited enhanced  
44 goblet cell differentiation and elevated IL-10 levels in mice. Taken together, these

45 findings identify the gut microbiome as a critical component of the anti- colitic effect  
46 of *T. spiralis* and gives beneficial insights into the processes by which  
47 helminth alleviates colitis.

48

49 **Author Summary**

50 Inflammatory bowel disease (IBD) encompasses Crohn's Disease and Ulcerative  
51 Colitis. It affects both children and adults. Reports have highlighted the potential use  
52 of helminths or their byproducts as a possible treatment for IBD. Accumulating  
53 evidence also suggests that the gut microbiota is a key factor in modulating IBD. In  
54 this study, we revealed the protective effect of a prior infection with *T. spiralis* on  
55 DSS- induced colitis in mice. Specifically, *T. spiralis* infection reshaped the gut  
56 microbiome of mice, resulting in an increased abundance of SCFA-producing bacteria  
57 *Muribaculum* and *unclassified\_Muribaculaceae* and thereby producing a larger  
58 amount of propionic acid. Furthermore, the gut microbiome modulated by *T. spiralis*  
59 exhibited enhanced goblet cell differentiation and elevated IL-10 levels, ultimately  
60 ameliorating experimental colitis. These findings suggest that the modulation of host  
61 microbiota during *T. spiralis* infection plays a crucial role in the suppression of colitis,  
62 and any intention-to-treat with helminth therapy should be based on the patient's  
63 immunological and microbiological response to the helminth.

64

65

66

67 **Introduction**

68 Inflammatory bowel disease (IBD) encompasses Crohn's Disease and Ulcerative  
69 Colitis. It affects both children and adults. The symptoms of the IBD are mild to  
70 severe and may threaten life, which not only include fever and diarrhea, but also  
71 abscess formation, stenosis, and the development of colitis- associated colorectal  
72 cancer [1, 2]. Multiple etiological factors, such as environmental factors, genetic  
73 background, and dysregulation of the immune system, are involved in IBD [3]. Since  
74 the middle of the twentieth century, the incidence of IBD has increased in the Western  
75 world, and now it has emerged in newly industrialized countries in Asia, South  
76 America and Middle East and has evolved into a global disease with rising prevalence  
77 in every continent [4].

78 Epidemiological studies have reported that within the last century helminths have  
79 gone from being ubiquitous to all but absent in developed countries. Further  
80 epidemiological investigations demonstrated that IBD is less prevalent in  
81 helminth-endemic countries [5]. Several different types of helminth infection in mice  
82 colitis models has also been shown some species, such as *Schistosoma mansoni* [6],  
83 *Heligmosomoides polygyrus* [7], *Trichinella spiralis* [8] and *Hymenolepis diminuta*  
84 [9], ameliorated the inflammatory reaction demonstrating certain anti- colitic effects.  
85 Most of these responses were characterized by an increase in Th2 immune response  
86 and regulatory T cells (Tregs), which consequently result in the secretion of  
87 regulatory cytokines that have anti-inflammatory characteristics.  
88 In addition to being associated with immune cells, the gut microbiota is considered a

89 crucial environmental factor in IBD [10]. Accumulating evidence suggests that the gut  
90 microbiota is a key factor in modulating the host immune system, influencing a  
91 predisposition to autoimmune diseases, including IBD [11]. A range of bacterial  
92 species, including *Lactobacillus*, *Bifidobacterium*, and *Faecali bacterium*, have  
93 shown this protective role via up-regulation of IL-10 production and down-regulation  
94 of pro-inflammatory cytokines. Moreover, *Clostridium* and *Bacteroides* species  
95 induced the expansion of Tregs to mitigate intestinal inflammation [12].  
96 Helminths coexist with the gut microbiota and their mammalian hosts, and can induce  
97 changes in the composition of the host's gut microbiome [13]. However, the potential  
98 influence and mechanism of helminth infections inducing alterations in the gut  
99 microbiota on the development of IBD has not yet been elucidated. In this study, we  
100 analyzed the intersection of helminth *T. spiralis* and gut bacteria in the regulation of  
101 colitis and related mechanisms. The data herein, show that the modulation of host  
102 microbiota by *T. spiralis* is essential to the suppression of colitis.

103

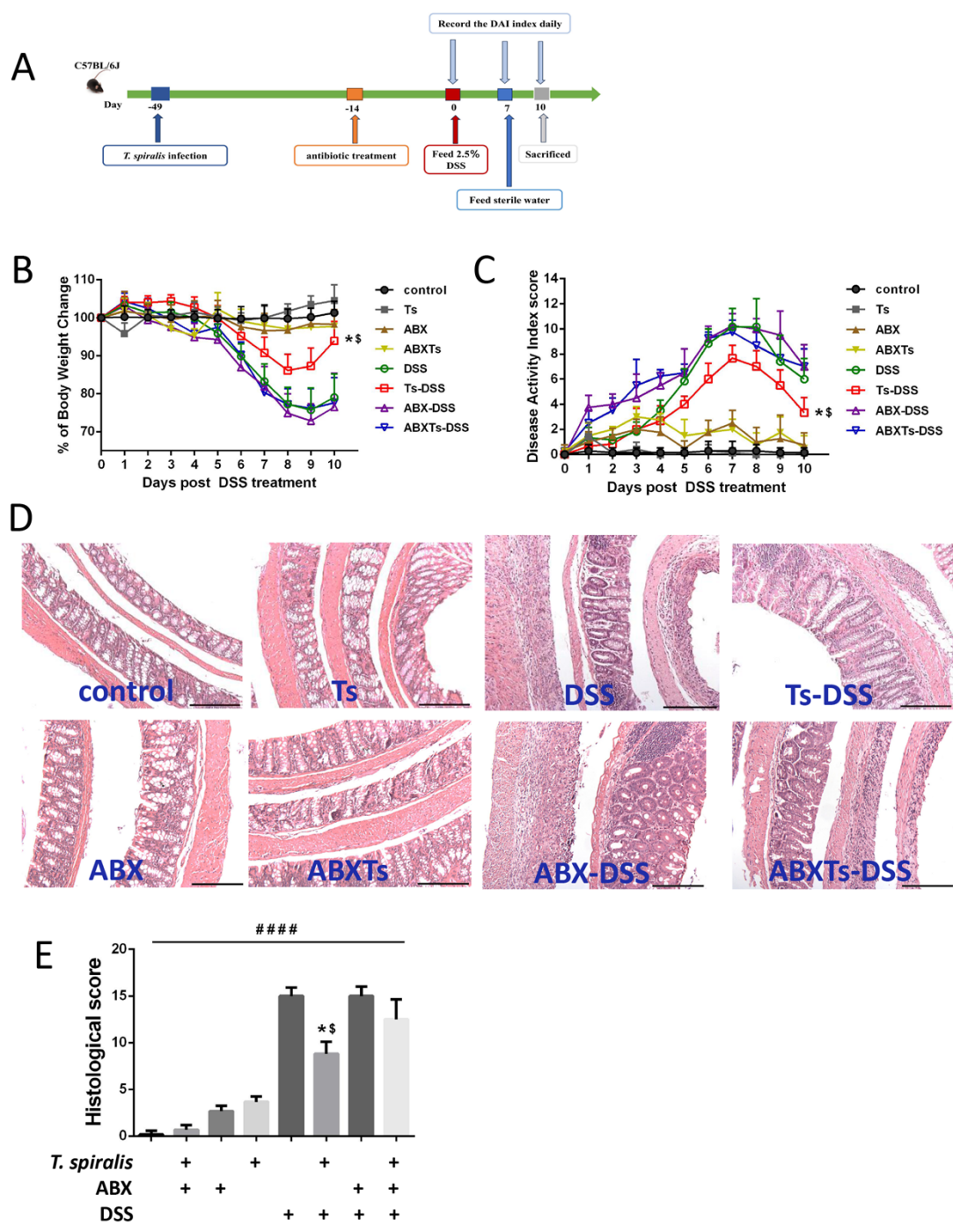
104 **Results**

105 **Antibiotics treatment abrogates *T. spiralis*-evoked suppression of colitis**

106 The possibility that the gut bacteria participated in *T. spiralis*- evoked suppression of  
107 colitis was tested with broad-spectrum antibiotics (**Fig 1A**). Data showed that mice  
108 present antibiotics (ABX) treatment during the induction of colitis exhibited an earlier  
109 onset of rectal bleeding and diarrhea compared to mice without ABX treatment (**S1**  
110 **Fig**). As expected, the DSS-treated group exhibited visible signs of inflammation

111 characterized by body weight loss, rectal bleeding, and diarrhea, leading to a  
112 significantly increased level of disease activity index (DAI) (**Fig 1B and 1C**), typical  
113 pathological changes, including epithelial erosion, edema, loss of the mucus layer,  
114 substantial polymorphonuclear infiltrate into the lamina propria, and increased  
115 histopathological score, and pre-infection of *T. spiralis* led to a significant decrease in  
116 weight loss and disease symptoms in DSS colitis (**Fig 1D and 1E**). However, the  
117 suppression of DSS- induced colitis evoked by infection with *T. spiralis* was absent in  
118 mice co-treated with ABX (**Fig 1B-1E**). The control, *T. spiralis* infection and ABX  
119 treatment alone mice showed no weight loss or microscopic damage of the colon.  
120 These results demonstrate that the gut bacteria participated in *T. spiralis*- evoked  
121 suppression of colitis.

**Fig 1**



123 **Fig 1. Broad-spectrum antibiotic treatment prevents *T. spiralis*-evoked inhibition**

124 **of colitis. (A)** *T. spiralis* infection, ABX treatment and DSS- induced colitis schedule,  
125 mice were orally gavaged with *T. spiralis* or PBS, 35 days later, some of the mice  
126 were treated with ABX daily for 14 days, then were given drinking water containing

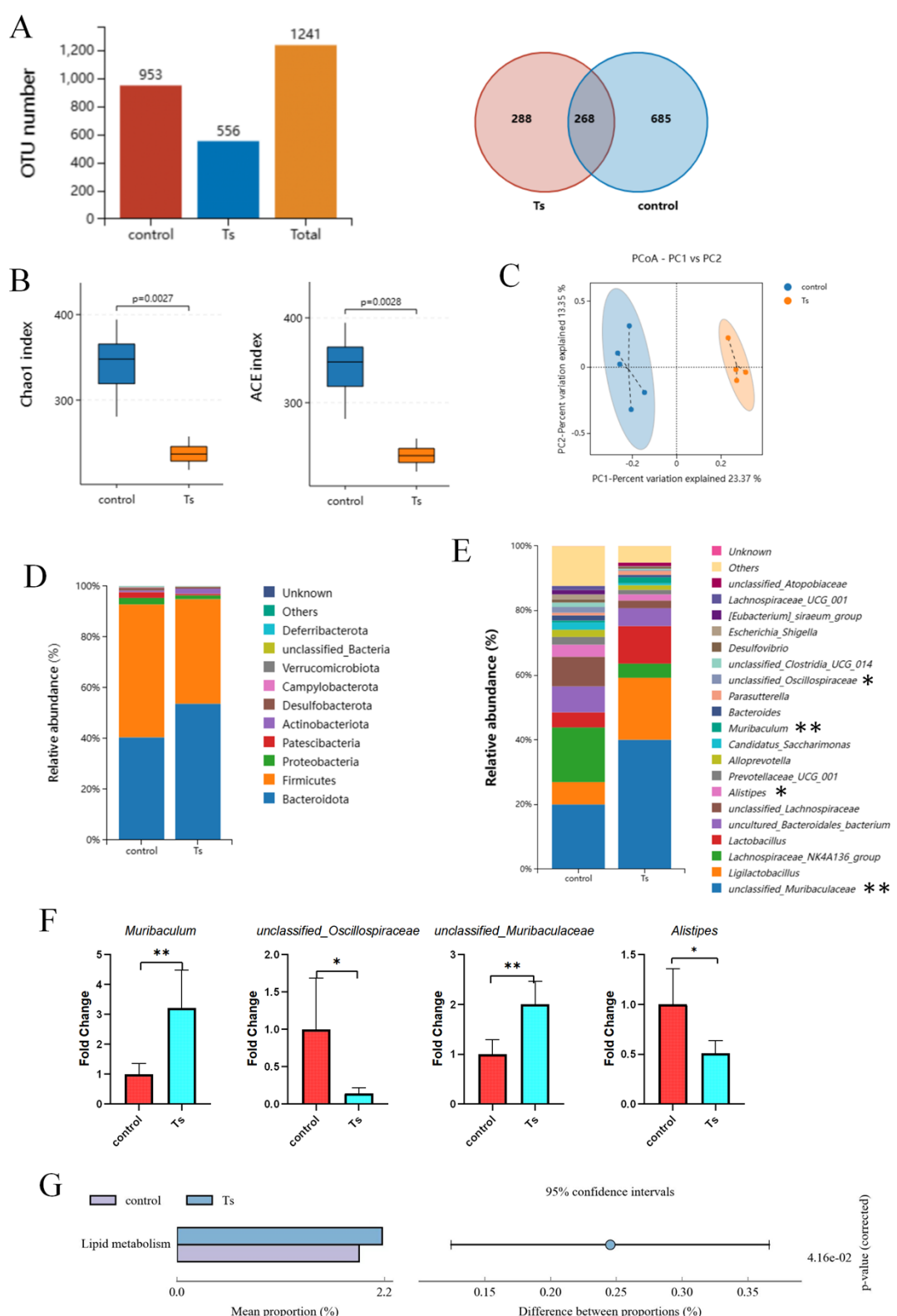
127 2.5% (wt/vol) DSS ad libitum for 7 days, and others left untreated as controls. After a  
128 further 3 days of distilled water fed, mice were sacrificed and samples were obtained  
129 and processed. **(B)** Weight change in percent. **(C)** The changes in disease activity  
130 index (DAI), scored from diarrhea, bleeding and body weight loss. **(D)** The  
131 histopathological changes in the colon tissues were examined by H&E staining, the  
132 black bar indicates 200  $\mu$ m. **(E)** Histopathological scores were determined for the  
133 colon tissue samples. The data shown are means  $\pm$  SD. Representative results from  
134 one out of three independent experiments with n = 5. \*, \$ P<0.05 compared to DSS  
135 and ABXTs-DSS, respectively; #####P < 0.0001 versus the respective control group.  
136 ABX: antibiotic cocktail of ampicillin (1g/L), vancomycin (0.5g/L), neomycin (1g/L),  
137 and metronidazole (1g/L) treated; ABXTs: *T. spiralis* infected and antibiotic treated;  
138 Ts: *T. spiralis* infected; DSS: DSS-induced colitis; Ts-DSS: *T. spiralis* infected and  
139 DSS induced colitis; ABX-DSS: antibiotic treated and DSS induced colitis;  
140 ABXTs-DSS: *T. spiralis* infected, antibiotic treated and DSS induced colitis  
141

#### 142 ***T. spiralis*- infected mice alters gut microbiome composition**

143 The influence of *T. spiralis* infection on mouse gut microbiota was determined using  
144 bacterial 16S rRNA gene sequencing. Venn diagram displayed decrease in operational  
145 taxonomic units (OTUs) in mice- infected with *T. spiralis* (**Fig 2A**). The Chao1 index  
146 and ACE index of  $\alpha$  diversity detection showed that *T. spiralis*- infected mice had a  
147 lower diversity of microbiota than control mice (**Fig 2B**). Besides,  $\beta$  diversity analysis  
148 of Principal Co-ordinates Analysis (PCoA) based on Binary-Jaccard demonstrated

149 that distinct clustering of microbiota composition between *T. spiralis*- infected mice  
150 and the control mice (**Fig 2C**). These data suggested that *T. spiralis* infection changed  
151 gut microbiota diversity and composition in mice. Then, we analyzed the bacterial  
152 profiles at the phylum and genus levels to further illuminate the difference of  
153 microbiota composition. At phylum level, Bacteroidota and Firmicutes were the  
154 dominant phyla followed by Proteobacteria, Patescibacteria, Actinobacteriota,  
155 Desulfobacteriota, Campylobacterota, Verrucomicrobiota and Deferribacterota (**Fig**  
156 **2D**). And data showed that *T. spiralis* infection increased the relative abundance of  
157 Bacteroidota and decreased the relative abundance of Firmicutes (**Fig 2D**). In terms of  
158 bacterial composition, our results showed that *T. spiralis* infection induced significant  
159 changes in gut microbiome composition, characterized by an increase in the  
160 abundance of the bacterial genus *Muribaculum* and *unclassified\_Muribaculaceae* and  
161 a decrease in the abundance of the bacterial genus *unclassified\_Oscillospiraceae* and  
162 *Alistipes* in the top 20 genera (**Fig 2E and 2F**). In addition to taxonomic composition,  
163 the functional profiles of microbial communities were predicted using the PICRUSt2  
164 software based on 16S rRNA gene- based microbial compositions. Significant  
165 differences were detected in KEGG pathways between the two groups, *T. spiralis*  
166 infection enhanced the function of lipid metabolism ( $P=0.0416$ ) (**Fig 2G**).

**Fig 2**



167

168 **Fig 2. *T. spiralis* infection changes gut microbiota composition in mice. Colon**

169 contents were collected and analyzed by using 16S rRNA gene sequencing. (A) The

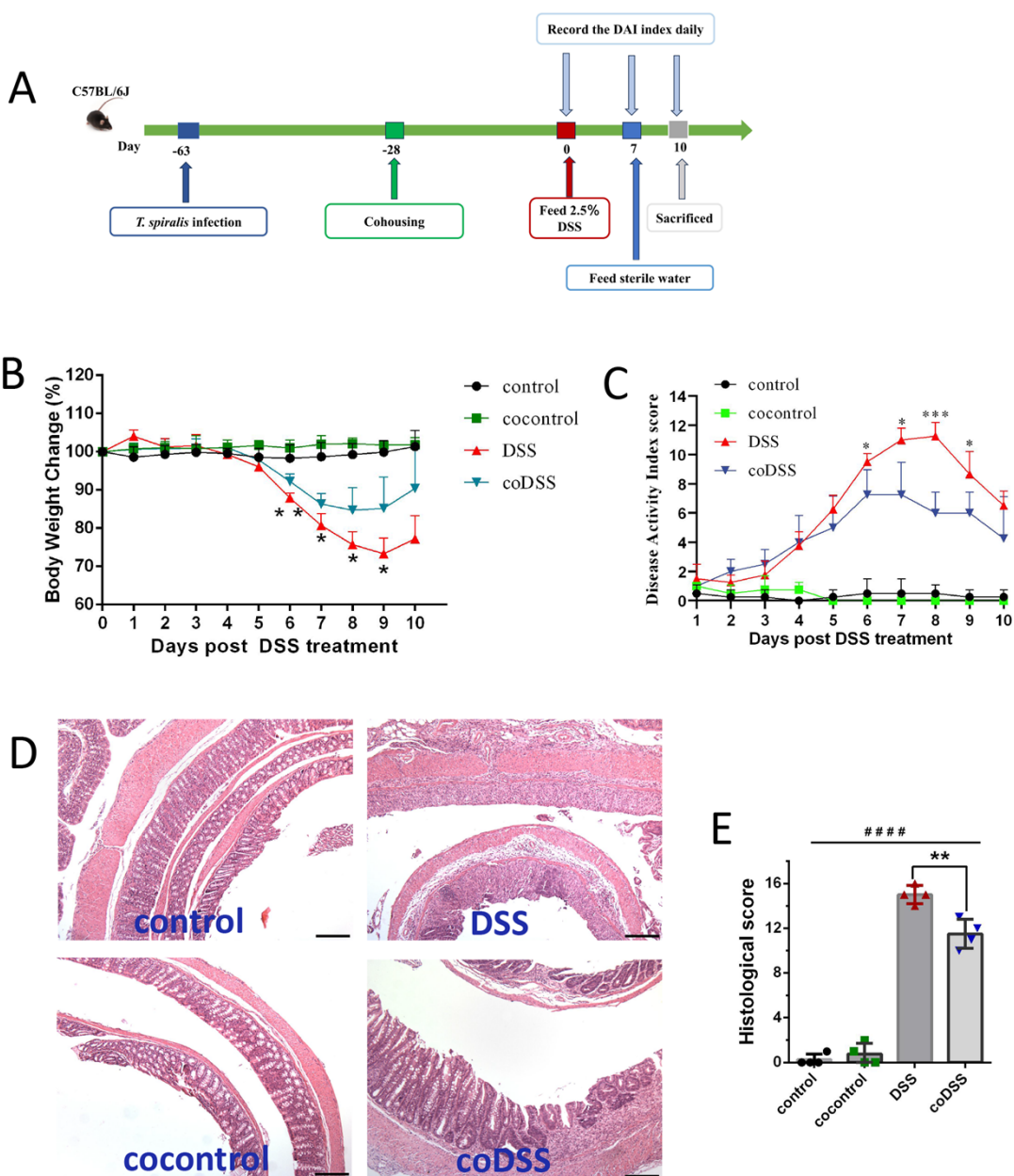
170 number of OTU, **(B)** Alpha diversity analysis (Chao 1 and ACE index), data are  
171 shown as Median, maximum, minimum, upper quartile and lower quartile. **(C)** Beta  
172 diversity analysis (PCoA based on Binary-Jaccard), **(D)** the relative abundance of  
173 OTUs at phylum and **(E)** the relative abundance of the top 20 genus in *T. spiralis*-  
174 infected mice and control mice. **(F)** The ratio of *Muribaculum*,  
175 *unclassified\_Muribaculaceae*, *unclassified\_Oscillospiraceae* and *Alistipes* in between  
176 groups, data are shown as the means  $\pm$  SD. \* $P < 0.05$ , \*\* $P < 0.001$  versus the control  
177 group. **(G)** Microbial community functions was predicted by PICRUSt2 using  
178 STAMP. Ts: *T. spiralis* infected

179

180 **Cohousing with *T. spiralis*- infected mice inhibits DSS- induced colitis**

181 To investigate whether *T. spiralis*- induced alterations in gut microbiota can improve  
182 colitis, a cohousing experiment was conducted. Mice were infected with *T. spiralis*  
183 for 35 days and then housed together with control mice. DSS- induced colitis was  
184 performed after mice were cohoused 4 weeks (**Fig 3A**). Results demonstrated that  
185 cohousing had no discernible impact on the development of DSS- induced colitis in  
186 mice present *T. spiralis* infection (**S2 Fig**). However, cohousing with *T. spiralis*-  
187 infected mice ameliorated the severity of DSS- induced colitis in mice without *T.*  
188 *spiralis*- infected, as evidenced by assessments of body weight, disease activity index,  
189 microscopic damage, and histopathology scores (**Fig 3B–3E**).

**Fig 3**



190

191 **Fig 3. Cohousing with *T. spiralis*- infected mice ameliorates the severity of colitis.**

192 (A) Infection, cohousing and DSS-induced colitis schedule. The mice were gavaged  
193 with *T. spiralis* 5 weeks prior to cohousing, and subsequently induced colitis after 4  
194 weeks of cohousing. (B) Weight change in percent. (C) The changes in disease  
195 activity index (DAI), scored from diarrhea, bleeding and body weight loss. (D) The  
196 histopathological changes in the colon tissues were examined by H&E staining, the

197 black bar indicates 200  $\mu$ m. (E) Histopathological scores were determined for the  
198 colon tissue samples. The data shown are means  $\pm$  SD. Representative results from  
199 one out of two independent experiments with n = 4. \*P <0.05, \*\*P <0.01, \*\*\*P  
200 <0.001 versus the DSS group. cocontrol: cohousing with *T. spiralis*- infected mice;  
201 DSS: DSS-induced colitis; co-DSS: cohousing with *T. spiralis*- infected mice and  
202 DSS-induced colitis

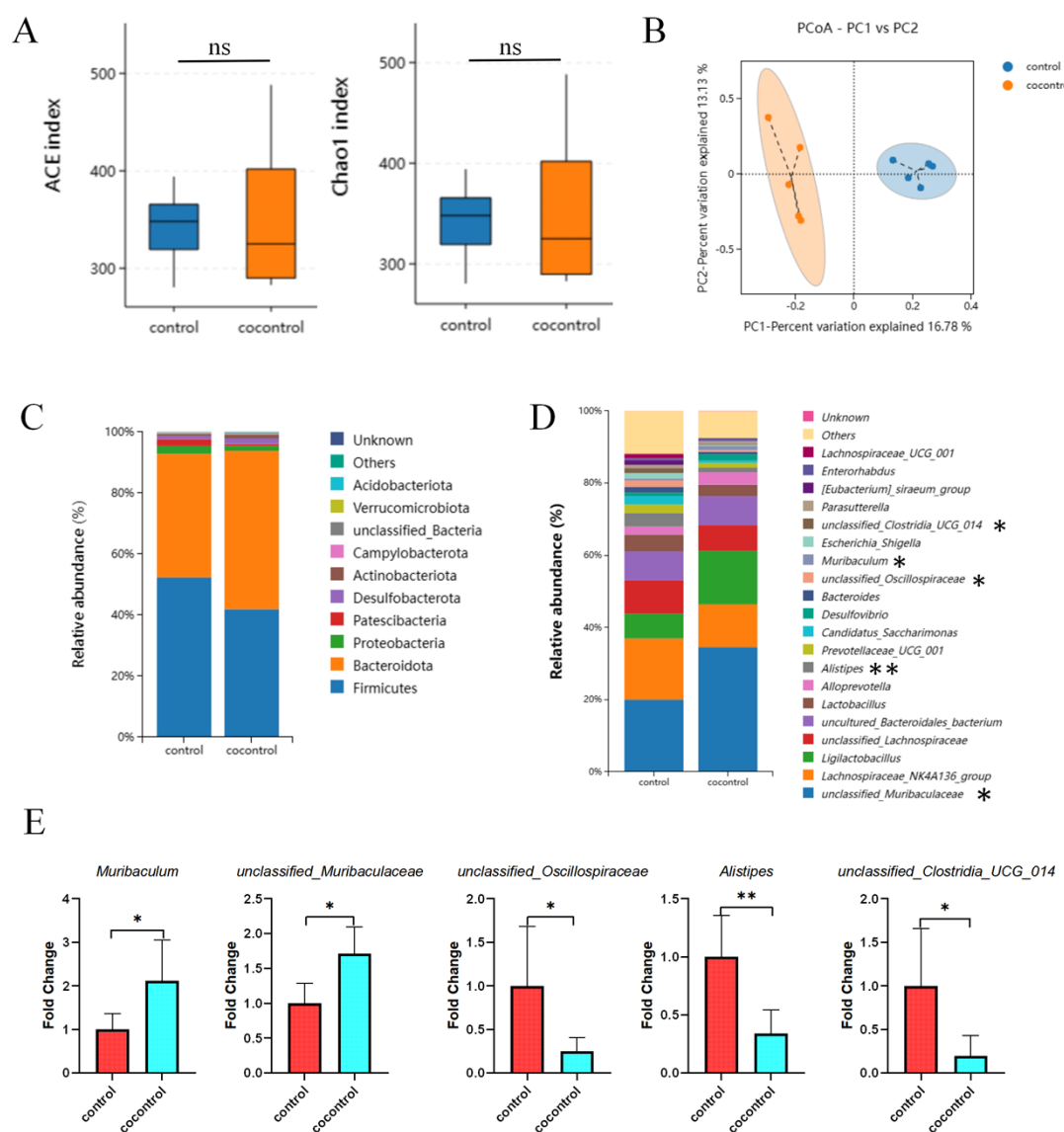
203

204 **Cohousing with *T. spiralis*- infected mice alters gut microbiome composition**

205 Subsequently, to investigate the potential impact of cohousing with *T. spiralis*-  
206 infected mice on gut microbiota composition, the control mice were housed in the  
207 same cage as *T. spiralis* -infected mice for a duration of four weeks. Then, mouse gut  
208 microbiota was determined using bacterial 16S rRNA gene sequencing. Results  
209 showed that although there was no statistically difference in Chao1 index and ACE  
210 index (**Fig 4A**); PCoA shown significantly different clustering of microbiota  
211 composition between control mice and cohousing control mice (**Fig 4B**). The data  
212 also indicated that mice cohousing with *T. spiralis*- infected mice exhibited similar  
213 alterations in the abundance of the bacterial phylum Bacteroidota and Firmicutes and  
214 genus *Muribaculum*, *unclassified\_Muribaculaceae*, *unclassified\_Oscillospiraceae* and  
215 *Alistipes* as those alteration in *T. spiralis*- infected mice (**Fig 4C-4E**). Additionally,  
216 there was a decrease in the relative abundances of *unclassified\_Clostridia\_UCG\_014*  
217 in cohousing control mice compared to control mice (**Fig 4E**). Furthermore, our data  
218 revealed no statistically significant differences in the Chao1 index, ACE index, PCoA,

219 phyla, genera, or cladogram obtained from the LEfSe analysis between cohoused and  
 220 *T. spiralis*- infected mice (S3 Fig). These results, therefore, demonstrate that  
 221 cohousing with *T. spiralis*- infected mice alters the gut microbiota composition.

**Fig 4**



222  
 223 **Fig 4. Cohousing with *T. spiralis*- infected mice induces alterations in the**  
 224 **composition of the gut microbiome. (A)** Alpha diversity analysis (Chao 1 and ACE  
 225 index), data are shown as Median, maximum, minimum, upper quartile and lower  
 226 quartile. **(B)** Beta diversity analysis (PCoA based on Binary-Jaccard). The relative

227 abundance of the top 10 phyla (**C**) and the top 20 genus (**D**) in mice. (**E**) The ratio of  
228 *Muribaculum*, *unclassified\_Muribaculaceae*, *unclassified\_Oscillospiraceae*,  
229 *Alistipesin* and *unclassified\_Clostridia\_UCG\_014* between groups control mice and  
230 mice cohousing with *T. spiralis*- infected mice, data are shown as the means  $\pm$  SD. \**P*  
231  $<0.05$ , \*\**P* $<0.001$  versus the control group. cocontrol: cohousing with *T. spiralis*-  
232 infected mice

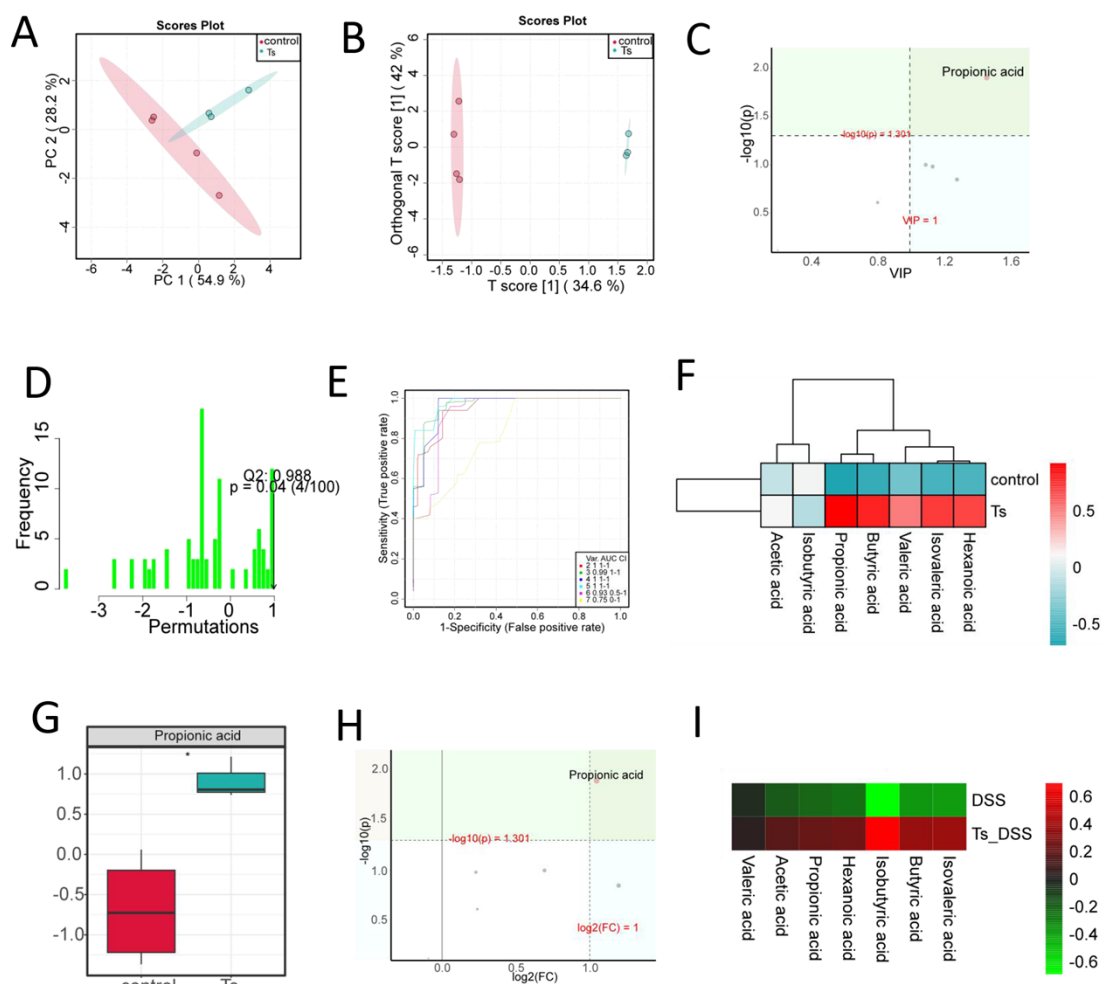
233

234 **Feces from *T. spiralis*- infected mice increase SCFAs**

235 The alterations in gut microbiota composition are invariably accompanied by changes  
236 in metabolites. To explore changes of intestinal metabolome after *T. spiralis* infection,  
237 GC-MS was used to analyze short-chain fatty acids (SCFAs) in fecal samples. The  
238 PCA score plot and OPLS-DA score plot showed that fecal samples from control  
239 mice and *T. spiralis*- infected mice could be easily divided into two distinct clusters  
240 (**Fig 5Aand 5B**). Based on VIP  $> 1$  and *P*  $< 0.05$  by OPLS-DA model, propionic acid  
241 was found as a potential biomarker (**Fig 5C**). Moreover, Permutation Test was  
242 performed to verify the validity of OPLS-DA model. And we found that Q2 actually  
243 observed was shown to the right of the random distribution and *P*  $< 0.05$ , which  
244 indicated that the OPLS-DA model had good differential stability and no fitting  
245 phenomenon (**Fig 5D**). Furthermore, Support Vector Machines were further employed  
246 to validate the difference of SCFAs concentration between control mice and *T.*  
247 *spiralis*- infected mice (**Fig 5E**), revealing an increase in hexanoic acid, isovaleric

248 acid, valeric acid, butyric acid and propionic acid in *T. spiralis*- infected mice  
249 compared to control mice (Fig 5F). Notably, the difference in propionic acid was  
250 found to be statistically significant, with a more than twofold increase observed in *T.*  
251 *spiralis*- infected mice compared to control mice (Fig 5G and 5H). Additionally, we  
252 also observed that hexanoic acid, isovaleric acid, valeric acid, butyric acid, propionic  
253 acid and acetic showed an increase in *T. spiralis*- infected DSS- treated mice  
254 compared to DSS- treated mice alone (Fig 5I).

**Fig 5**



255  
256 **Fig 5. Feces from *T. spiralis*- infected mice contain increase amounts of**  
257 **short-chain fatty acids (SCFAs). (A) PCA score plot and (B) OPLS-DA score plot**

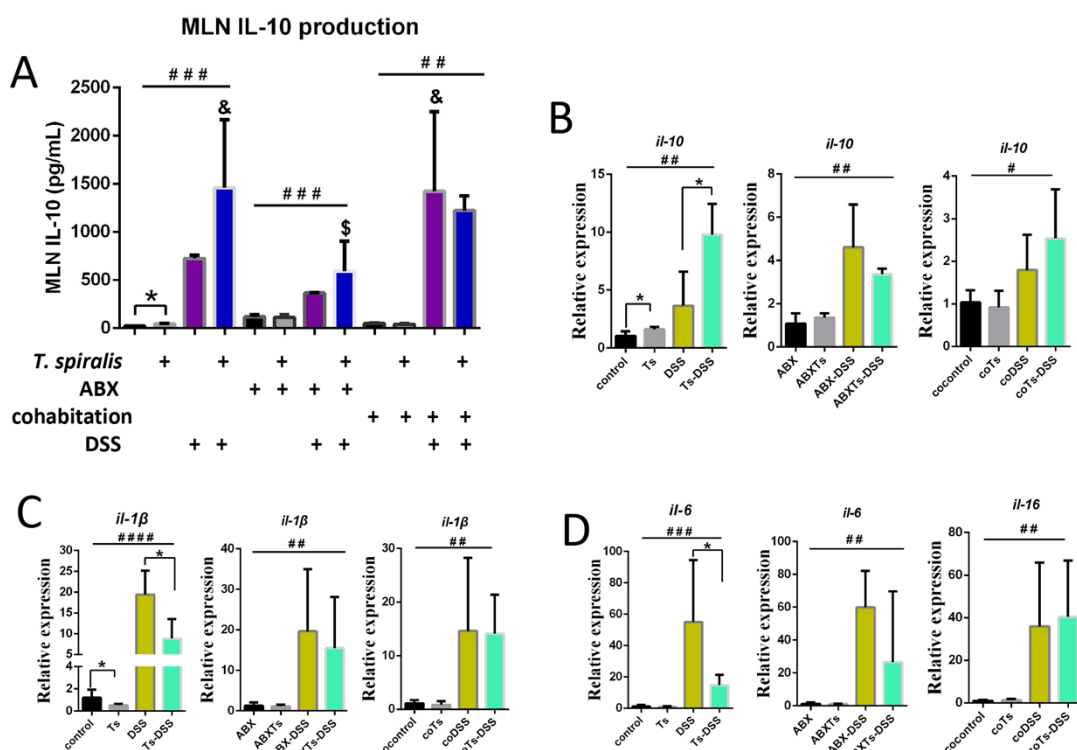
258 shown the difference of control mice and *T. spiralis* -infected mice. **(C)** Volcano map  
259 of SCFAs by OPLS-DA model. The abscissa represents Value Importance in  
260 Projection (VIP); the ordinate represents the level of significant difference ( $-\log_{10}$   
261 (p)). **(D)** Permutation Test was performed to verify the validity of OPLS-DA model.  
262 **(E)** Receiver Operating Characteristic (ROC) curve by Support Vector Machines  
263 (SVM). **(F)** Heat-map of SCFAs between control mice and *T. spiralis*- infected mice.  
264 **(G)** Box plot of propionic acid, data are shown as Median, maximum, minimum,  
265 upper quartile and lower quartile. **(H)** Volcano map of SCFAs. The abscissa  
266 represents the logarithm of the relative content fold change ( $\log_2(\text{FC})$ ) of a  
267 metabolite in two groups; the ordinate represents the level of significant difference  
268 ( $-\log_{10}(p)$ ). **(I)** Heat-map of SCFAs between DSS- treated alone group (DSS) mice  
269 and *T. spiralis*- infected DSS- treated group (Ts\_DSS). \* $P < 0.05$  compared to control  
270

271 ***T. spiralis* infection alters immune responses and epithelial barrier properties in  
272 DSS- induced colitis mice by modulating the gut microbiome**

273 To explore for the anti-inflammatory role of *T. spiralis* infection or cohousing with  
274 infected mice, we investigated tissue immuno- regulatory environment in mice.  
275 Lymphocyte were prepared from MLN and stimulated by anti-CD3 antibody. IL-10 in  
276 the supernatants were analyzed by ELISA kits. Results showed that the IL-10  
277 production in MLN was upregulated when the mice were induced colitis by DSS in  
278 the presence or absence of *T. spiralis* infection, antibiotic treatment, or cohousing ( $P$

279 <0.05) (**Fig 6A**). Besides, during DSS- induced colitis, *T. spiralis*- infected mice and  
280 cohousing mice exhibited a significantly elevated level of IL-10 production in the  
281 MLN compared to DSS- treated mice alone; however, the increase of IL-10  
282 production in *T. spiralis*- infected mice was abolished upon antibiotic treatment (**Fig**  
283 **6A**). Additionally, the expression level of IL-10, IL-1 $\beta$  and IL-6 were assessed in  
284 colon tissue using RT-qPCR. Results revealed an upregulation of IL-10 expression  
285 and a downregulation of IL-1 $\beta$  and IL-6 expression in *T. spiralis*- infected mice  
286 compared to DSS- treated mice alone during the induction of colitis (**Fig 6B-6D**).  
287 However, the differences in the expressions of these cytokines disappeared when the  
288 mice were treated with antibiotics or cohoused with *T. spiralis*- infected mice (**Fig**  
289 **6B-6D**).

## Fig 6

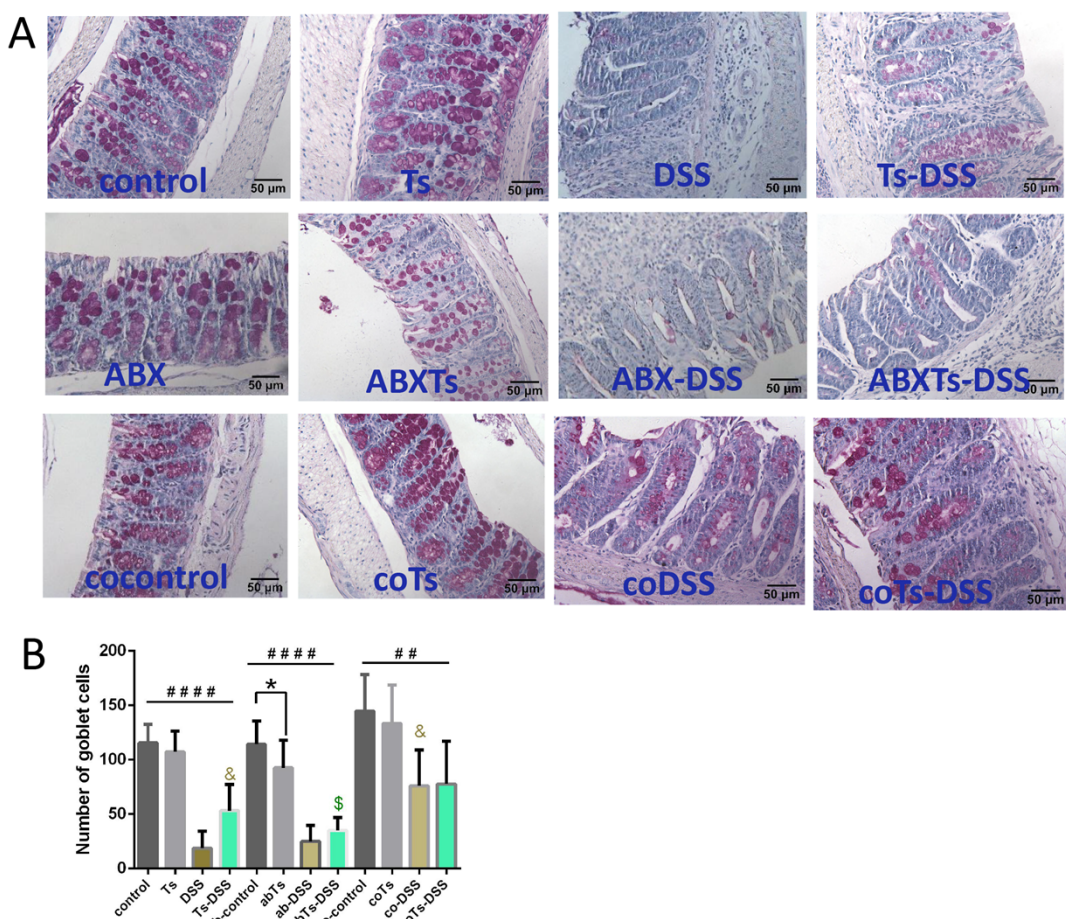


290

291 **Fig 6. *T. spiralis* infection results in the regulation of both pro-inflammatory and**  
292 **immunoregulatory cytokine responses during DSS- induced colitis by**  
293 **modulating the gut microbiome.** Mice infected with *T. spiralis* were subjected to  
294 antibiotic treatment or cohousing with control mice, followed by administration with  
295 or without DSS. **(A)** Lymphocytes were prepared from MLN and stimulated by  
296 anti-CD3 antibody. IL-10 in the supernatants were analyzed by ELISA kits. **(B-D)**  
297 The colonic tissues were collected; and the mRNA expression of IL-10, IL-1 $\beta$  and  
298 IL-6 was determined using RT-qPCR. The data shown are means  $\pm$  SD (n = 4-5 mice  
299 per group) from one of three experiments performed showing similar results. \*P  
300  $<0.05$  between the indicated groups; #P  $<0.05$ , ##P  $<0.01$ , ###P  $<0.001$ , #####P  
301  $<0.0001$  versus the respective control group; & P  $<0.05$  versus the DSS group; \$ P  
302  $<0.05$  versus the Ts-DSS group. ABX: antibiotic treated; Ts, *T. spiralis* infected;  
303 ABXTs: *T. spiralis* infected and antibiotic treated; DSS: DSS induced colitis; Ts-DSS:  
304 *T. spiralis* infected and DSS induced colitis; ABX-DSS: antibiotic treated and DSS  
305 induced colitis; ABXTs-DSS: *T. spiralis* infected, antibiotic treated and DSS induced  
306 colitis; cocontrol: cohousing with *T. spiralis* infected mice; coTs: *T. spiralis* infected  
307 and cohoused; coDSS: cohousing with *T. spiralis* infected mice and DSS induced  
308 colitis; coTs-DSS: *T. spiralis* infected, cohoused and DSS induced colitis  
309  
310 To further determine whether *T. spiralis* infection could affect colonic goblet cell  
311 response, contributing to the observed protection, Periodic Acid Schiff (PAS) staining  
312 was performed on the mouse colonic sections. Our results demonstrated a significant

313 decrease in the number of goblet cells (PAS+ cells) in the colons of DSS- treated mice  
314 compared to their respectively control mice ( $P < 0.05$ ) (**Fig 7**). During DSS- induced  
315 colitis, *T. spiralis*- infection and cohousing resulted in a significant increase in goblet  
316 cell numbers compared to DSS- treated mice alone; however, this increase was  
317 abolished upon antibiotic treatment (**Fig 7A and 7B**). Furthermore, administration of  
318 antibiotics resulted in a decrease in the number of colonic goblet cells in mice infected  
319 with *T. spiralis* compared to those receiving antibiotic treatment alone. Taken  
320 together, these results demonstrate that *T. spiralis* infection alters immune responses  
321 and epithelial barrier properties in DSS- induced colitis mice by modulating the gut  
322 microbiome.

**Fig 7**



323

324 **Fig 7. *T. spiralis* infection modulates epithelial barrier properties during DSS-  
325 induced colitis by modulating the gut microbiome.** Mice infected with *T. spiralis*  
326 were subjected to antibiotic treatment or cohousing. (A) Goblet cells were stained as  
327 the average score of 10 random fields from each mouse. The data shown are means  $\pm$   
328 SD (n = 4-5 mice per group). \*P < 0.05 between the indicated groups; ##P < 0.01,  
329 #####P < 0.0001 versus the respective control group; & P < 0.05 versus the DSS group;  
330 \$ P < 0.05 versus the Ts-DSS group. ABX: antibiotic treated; Ts, *T. spiralis* infected;  
331 ABXTs: *T. spiralis* infected and antibiotic treated; DSS: DSS induced colitis; Ts-DSS:  
332 *T. spiralis* infected and DSS induced colitis; ABX-DSS: antibiotic treated and DSS

334 induced colitis; ABXTs-DSS: *T. spiralis* infected, antibiotic treated and DSS induced  
335 colitis; cocontrol: cohousing with *T. spiralis* infected mice; coTs: *T. spiralis* infected  
336 and cohoused; coDSS: cohousing with *T. spiralis* infected mice and DSS induced  
337 colitis; coTs-DSS: *T. spiralis* infected, cohoused and DSS induced colitis

338

339 **Discussion**

340 Helminth infections are known to be powerful modulators of the human immune  
341 response, and numerous studies now highlight the effects may have on human  
342 infectious, inflammatory, and metabolic diseases [14]. The helminth *Trichinella*  
343 *spiralis* is the causative agent of trichinosis. Humans contract *T. spiralis* by  
344 consuming uncooked meat that carries encysted *T. spiralis* larvae in muscle tissue;  
345 then larvae are released by gastric fluids, molt and mature into adult worm. The  
346 female adult worms release newborn larvae after copulation, which travel through the  
347 circulatory system to reach skeletal muscle cells [14, 15]. As a helminth with all  
348 stages of larval and adult development occurring within the same host organism, *T.*  
349 *spiralis* is one of the most successful parasitic symbionts, ensuring its survival and  
350 immune dialogue with the host [16]. Multiple studies have confirmed the  
351 anti-inflammatory effect of *T. spiralis* in animal models. Chronic infection with *T.*  
352 *spiralis* can mediate protection against allergic asthma, *Pseudomonas aeruginosa*-  
353 induced pneumonia, influenza or respiratory syncytial virus- associated pathologies in  
354 mice [15, 17-19]. Evidence also indicates that *T. spiralis* infection attenuates  
355 *Citrobacter rodentium*, acetic acid, trinitrobenzesulfonic acid or DSS- induced

356 colonic damage [8, 20-23]. However, the potential influence and mechanism of *T.*  
357 *spiralis* infection inducing alterations in the gut microbiota on the development of  
358 IBD is still largely undetermined. In this study, we analyzed the intersection of *T.*  
359 *spiralis* and gut bacteria in the regulation of colitis and related mechanisms by  
360 infecting mice with *T. spiralis*, administering broad-spectrum antibiotics to mice, or  
361 cohousing mice with *T. spiralis*-infected counterparts. Our findings revealed that prior  
362 infection with *T. spiralis* or cohousing with *T. spiralis*-infected mice could ameliorate  
363 DSS- induced colitis through an increase abundance of SCFA-producing bacteria.  
364 Consistent with previous effects, our current study demonstrated that infection with  
365 *T. spiralis* significantly reduced disease activity index, ameliorated clinical symptoms,  
366 and improved colonic histological damage in mice with DSS- induced colitis.  
367 However, treatment with broad spectrum antibiotics was found to prevent the  
368 inhibition of colitis evoked by *T. spiralis* infection, suggesting that lack of inhibition  
369 of colitis was linked to the microbiota. Subsequently, we employed 16S rRNA gene  
370 sequencing to investigate the impact of *T. spiralis* infection on gut microbiota and  
371 observed significant alterations in both diversity and composition. *T. spiralis* infection  
372 led to an increase in the abundance of Bacteroidota while decreasing the abundance of  
373 Firmicutes at the phylum level. Specifically, characterized by an increase in the  
374 abundance of the bacterial genus *Muribaculum* and *unclassified\_Muribaculaceae* and  
375 a decrease in the abundance of the opportunistic pathogens [24, 25] bacterial genus  
376 *unclassified\_Oscillospiraceae* and *Alistipes* in the top 20 genera. It is worth noting  
377 that the differential effects of feces from *T. spiralis*- infected mice may also arise

378 from variations in gut bacteria composition due to factors such as animal source,  
379 housing conditions, diet or duration of infection [26-28]. Dissecting the role of the  
380 microbiota in the anti-colitic evoked by *T. spiralis* infection, cohousing the control  
381 mice with *T. spiralis* infection mice conferred protection from DSS- induced colitis.  
382 Furthermore, cohousing control mice exhibited similar changes in the bacterial genera  
383 *Muribaculum*, *unclassified\_Muribulaceae*, *unclassified\_Oscillospiraceae*, and  
384 *Alistipes* as those observed in *T. spiralis*- infected mice. *Muribaculum* is a major  
385 forager of mucin monosaccharides, which could impede the colonization of  
386 *Clostridioides difficile* [29]. The infection of *T. spiralis* significantly enhanced the  
387 relative abundance of *Muribaculum*, thereby potentially impeding pathogen  
388 colonization and maintaining intestinal homeostasis simultaneously. Meanwhile, both  
389 *Muribaculum* and *unclassified\_Muribulaceae* belong to the family Muribulaceae  
390 [30], whose abundance exhibits a negative correlation with gut inflammation [31-33].  
391 Our observations align with previous studies showing a robust interaction between *T.*  
392 *spiralis*- modulated *Muribaculum* and *unclassified\_Muribulaceae* and IBD. In  
393 addition to taxonomic composition, the functional profiling of microbial communities  
394 revealed a significant enhancement in lipid metabolism function within gut bacteria  
395 derived from *T. spiralis*- infected mice.  
396 SCFAs are metabolized by intestinal bacteria from a fiber-rich diet that is otherwise  
397 indigestible, and primarily consist of acetic acid, propionic acid and butyric acid [34].  
398 A growing body of research has indicated that SCFAs play critical roles in IBD  
399 [35-38]. Our results provide evidence indicating that *T. spiralis*- enriched

400 *Muribaculum* and *unclassified\_Muribulaceae* are correlated with enhanced  
401 production of SCFAs [30], especially propionic acid, which has been demonstrated to  
402 possess functions in reducing the relapse rate and disability progression of multiple  
403 sclerosis by increasing expression of Treg-cell-inducing genes, such as IL-10 [39], as  
404 well as alleviating intestinal inflammation by enhancing goblet cell differentiation and  
405 mucus function [40].

406 IL-10 is a pre-dominantly anti-inflammatory cytokine with an essential role in  
407 maintaining gastrointestinal homeostasis, which potently inhibits production of most  
408 inducible chemokines that are involved in inflammation [41]. Several helminthes  
409 attenuate colitis in DSS models by inducing anti-inflammatory cytokine expression  
410 and downregulating pro-inflammatory cytokines expression [7, 9]. Consistent with  
411 previous studies, helminth *T. spiralis* demonstrated a significant upregulation of IL-10  
412 and downregulation of IL-1 $\beta$  and IL-6. Interestingly, mice cohousing with *T. spiralis*-  
413 infected mice also exhibited a significantly heightened level of IL-10 production,  
414 while the discrepancy in IL-10 production was eliminated upon administration of  
415 antibiotics to the mice. These findings suggest a robust interplay between *T. spiralis*-  
416 modulated microbiota and anti-inflammatory cytokine IL-10.

417 Goblet cells are recognized as key regulators of intestinal barrier homeostasis and  
418 play a crucial role in defending against enteric pathogen infections [42]. Alterations  
419 of goblet cell number and mucus formation are associated with the pathogenesis and  
420 progression of IBD, including ulcerative colitis and Crohn's disease [40]. In this study,  
421 we identified the critical role of *T. spiralis*- modulated microbiota in alleviating DSS-

422 induced colitis and enhancing goblet cell proportions. During DSS- induced colitis, *T.*  
423 *spiralis* infection and cohousing resulted in a significant increase in goblet cells;  
424 however, this increase was abolished after antibiotic treatment. These findings suggest  
425 a robust interplay between *T. spiralis*- modulated microbiota and goblet cell  
426 proportions. However, the role of SCFAs in mediating the beneficial effects of *T.*  
427 *spiralis*- modulated microbiota on colitis remains a crucial question that requires  
428 further investigation.

429 In conclusion, we revealed the protective effect of a prior infection with *T. spiralis* on  
430 DSS- induced colitis in mice. Specifically, *T. spiralis* infection reshaped the gut  
431 microbiome of mice, resulting in an increased abundance of SCFA-producing bacteria  
432 *Muribaculum* and *unclassified\_Muribaculaceae* and thereby producing a larger  
433 amount of propionic acid. Furthermore, the gut microbiome modulated by *T. spiralis*  
434 exhibited enhanced goblet cell differentiation and elevated IL-10 levels, ultimately  
435 ameliorating experimental colitis. These findings suggest that the modulation of host  
436 microbiota during *T. spiralis* infection plays a crucial role in the suppression of colitis.  
437 Our research gives beneficial insights into the processes by which helminth alleviates  
438 colitis.

439

#### 440 **Materials and methods**

##### 441 **Experimental animals**

442 Pathogen-free, 6-week-old female C57BL/6J mice were purchased from  
443 GemPharmatech (Jiangsu, China). They were fed autoclaved food and water. All of

444 the animal experiments were approved by the Zhengzhou University Life Science  
445 Ethics Committee (No. ZZUIRB GZR 2021–0044).

446

447 **Helminth infection and DSS-Induced Colitis**

448 The helminth parasite *T. spiralis* (ISS534) was collected as previously described [43].  
449 Four groups of mice (5 mice per group, include control: PBS control group, Ts: *T.*  
450 *spiralis*- infected group, DSS: DSS- induced colitis group, and Ts-DSS: *T. spiralis*-  
451 infected DSS- induced colitis group) were used. Three independent experiments were  
452 performed. *T. spiralis* infected groups were administered 100 muscle larvae orally by  
453 gavage with a 21-gauge feeding needle. Control group was gavaged with PBS at the  
454 same time. *T. spiralis* infection was incubated for a period of 35 days prior to  
455 treatment of the mice with DSS. Experimental colitis was induced as previous  
456 study[43]. A 2.5% (wt/vol) solution of DSS (M.W. 36000–50000 kDa; MP  
457 Biomedicals, Cat. no. 106110) were administered to mice as a substitute for  
458 autoclaved water for 7 days. At day 7 post DSS administration, the DSS solution was  
459 replaced by autoclaved water. After a further 3 days of water fed, mice were sacrificed  
460 and samples were obtained and processed. Clinical parameters including body weight,  
461 bleeding, and stool consistency were recorded daily to calculate the clinical disease  
462 score (disease activity index, DAI) [44].

463

464 **Antibiotic treatment of mice**

465 Mice were infected with *T. spiralis* for 35 days, then treated with a broad-spectrum

466 cocktail of antibiotics (ABX: drinking water, ampicillin (1g/L), vancomycin (0.5g/L),  
467 neomycin (1g/L), and metronidazole (1g/L)) daily for 14 days to deplete the gut  
468 microbiota. To evaluate the role of gut microbiota in helminth-ameliorated colitis,  
469 four groups of mice (3-4 mice per group, include ABX: antibiotic treatment control  
470 group, abTs: *T. spiralis*- infected antibiotic-treated group, ab-DSS: antibiotic-treated  
471 DSS-induced colitis group, and abTs-DSS: *T. spiralis*- infected antibiotic- treated and  
472 DSS-induced colitis group) were used. Two independent experiments were performed.  
473 DSS induced colitis was performed 2 weeks after antibiotic treatment.

474

#### 475 **Cohousing of mice**

476 To investigate whether helminth-induced alterations in gut microbiota can improve  
477 colitis, a cohousing experiment was conducted between helminth- infected mice and  
478 control mice. Mice were infected with *T. spiralis* for 35 days and then housed together  
479 with PBS- treated control mice. Four groups of mice (4 mice per group, include  
480 cocontrol: cohoused control group, coTs: *T. spiralis* infected and co-housed group,  
481 co-DSS: cohoused and DSS-induced colitis group, and coTs-DSS: *T. spiralis*-infected,  
482 cohoused, and DSS-induced colitis group) were used. Two independent experiments  
483 were performed. DSS induced colitis was performed 4 weeks after cohousing.

484

#### 485 **Histopathological examinations**

486 A 0.5-1.0 cm colon piece (cecum side) was collected for the measurement of tissue  
487 cytokine expression by using RT-qPCR, the rest of the colon tissue was cut

488 longitudinally and rolled into the shape of a Swiss roll. The colons were fixed in 4%  
489 formaldehyde and embedded in paraffin. The process tissues were sectioned into 5  $\mu$ m  
490 thick slices and stained with hematoxylin and eosin (H&E). The extent of colonic  
491 inflammatory damage was assessed using the scoring system described by Wang et al  
492 [45]. Goblet cells were stained with periodic acid-schiff (PAS) following  
493 manufacturer instructions, and the number of goblet cells per field in the colon were  
494 quantified.

495

#### 496 **Lymphocyte isolation and IL-10 production measurement**

497 Mice were sacrificed 10 days after DSS treatment. Lymphocyte suspensions were  
498 prepared from mesenteric lymph nodes (MLN) by pressing the cells through a 70- $\mu$ M  
499 nylon cell strainer (Falcon; BD Labware) in complete Dulbecco's modified Eagle's  
500 medium (cDMEM) (10% fetal calf serum, , 2mM L-glutamine, 100U of penicillin/mL,  
501 100 $\mu$ g of streptomycin/mL, 1% nonessential amino acids, and 110mg/L sodium  
502 pyruvate, 4.5g/L D-Glucose). Red blood cells were lysed. Cells (1x10<sup>6</sup> cells/mL) were  
503 cultured in a 48-well plate pre-coated with anti-CD3 monoclonal antibody (BD  
504 Pharmingen, 5 $\mu$ g/mL), and culture supernatants were collected after 72h  
505 of stimulation and stored at -80°C until assayed for cytokine production. IL-10 in the  
506 supernatants were analyzed by ELISA kits (Proteintech, KE10008).

507

#### 508 **RNA extraction and RT-qPCR**

509 RNA extraction was performed by lysing 50 mg of mouse colon tissue samples with  
510 Trizol reagent (Invitrogen, USA) and then converted to cDNA. Quantitative real-time  
511 reverse-transcription PCR (RT-qPCR) assays were performed on a 7500 Fast  
512 Real-Time PCR system (Applied Biosystems, USA). The primer sequences were  
513 listed in **S1 Table**. The relative mRNA expression levels of the target genes were  
514 normalized to those of the indicated housekeeping gene (GAPDH) and were  
515 quantified using the comparative Ct method and the formula  $2^{-\Delta\Delta CT}$ .

516

### 517 **Gut microbiome analysis**

518 Fecal samples were collected from the control mice, *T. spiralis* infected mice and  
519 cohousing mice. DNA was extracted from fecal samples and added spike-in DNA at a  
520 certain ratio. Based on 16s v3+v4\_b, primes were designed as F:  
521 ACTCCTACGGGAGGCAGCA; R: GGACTACHVGGGTWTCTAAT and the  
522 sequencing adapter was added at the end of the primers. PCR amplification was  
523 carried out, and the products were purified, quantified and normalized to form a  
524 sequencing library. Qualified libraries were sequenced using Illumina Novaseq 6000  
525 for paired-end reads. The raw reads were preconditioned using Trimmomatic v0.33,  
526 cutadapt 1.9.1, Usearch v10 and so on to get high-quality reads. Operational  
527 taxonomic units (OTUs) based on  $\geq 97\%$  sequence similarity were obtained by using  
528 the dada2 method included in the QIIME2 software. Alpha diversity (Chao 1 and  
529 ACE index) and Beta diversity (PCoA based on Binary-Jaccard) were analyzed by

530 using QIIME2 software. Using SILVA as a reference database and Naive Bayesian  
531 classifier for taxonomic annotation of feature sequences.

532

533 **Measurement of fecal short-chain fatty acids (SCFAs)**

534 Fecal samples were thawed on ice. 200 mg of sample was suspended with 50 uL of  
535 20% phosphoric acid, added 4-methylvaleric acid to a final concentration of  
536 500ug/mL as internal standard, mixed for 2 min and centrifuged at 14000 g for 20 min.

537 Su pernatant was analyzed by Gas Chromatography-Mass Spectrometry (GC-MS).

538 Metabolites were separated on gas chromatography system with Agilent DB-FFAP  
539 capillary column (30m × 250um × 0.25um) and then performed mass spectrometry by  
540 5977B MSD Agilent. Area of chromatographicpeak and retention time were extracted  
541 by MSD ChemStation software. The concentration of SCFAs was calculated by  
542 drawing standard curve. This metabolome analysis workflow was based on  
543 MetaboAnalystR [46].

544

545 **Statistical analysis**

546 All data were statistically analyzed using GraphPad Prism 8 and presented as mean ±  
547 SD. Statistical differences were determined using a two-tailed Student t test or  
548 One-way ANOVA with SPSS 21.0 software. A *P* value < 0.05 was considered  
549 significant.

550

551 **Supporting information**

552 **S1 Fig. Mice present ABX treatment during the induction of colitis exhibits an**  
553 **earlier onset of (A) diarrhea and (B) rectal bleeding compared to mice without**  
554 **ABX treatment.** The data shown are means  $\pm$  SD. Representative results from one  
555 out of two independent experiments with  $n = 5$ . \* $P < 0.05$  compared to DSS group.  
556 DSS: DSS- induced colitis; ABX-DSS: antibiotic- treated and DSS- induced colitis

557

558 **S2 Fig. Cohousing has no impact on the DSS-induced colitis in mice present *T.***  
559 ***spiralis* infection. (A)** Weight change in percent. **(B)** The changes in disease activity  
560 index (DAI), scored from diarrhea, bleeding and body weight loss. **(C)** The  
561 histopathological changes were examined by H&E staining, the black bar indicates  
562 200  $\mu$ m. **(D)** Histopathological scores. The data shown are means  $\pm$  SD.  
563 Representative results from one out of two independent experiments with  $n = 4$ . Ts, *T.*  
564 *spiralis*- infected; coTs: *T. spiralis*- infected and cohoused; Ts-DSS: *T. spiralis*-  
565 infected and DSS- induced colitis; coTs-DSS: *T. spiralis*- infected, cohoused and  
566 DSS- induced colitis

567

568 **S3 Fig. The gut microbiota composition in mice becomes consistent when**  
569 **cohousing of control and *T. spiralis*- infected mice. (A)** Alpha diversity analysis  
570 (Chao 1 and ACE index), data are shown as median, maximum, minimum, upper  
571 quartile and lower quartile. **(B)** Beta diversity analysis (PCoA based on  
572 Binary-Jaccard). The relative abundance of the top 10 phyla **(C)** and the top 20 genus  
573 **(D)** in cohousing control mice and cohousing *T. spiralis*- infected mice. **(E)**

574 Cladogram was obtained from the LEfSe analysis when the effect size threshold of  
575 LDA was set to 3.5. cocontrol: cohousing with *T. spiralis*- infected mice; coTs: *T.*  
576 *spiralis* infected and cohoused

577

578 **S1 Table Primers used for qRT-PCR analysis**

579

580 **Funding**

581 This work was supported by grants from Medical Science and Technology project of  
582 Henan Province (LHGJ20200372).

583

584 **Data Availability**

585 The datasets used and analyzed in this article are available from the corresponding author upon  
586 reasonable request.

587

588 **Competing interests**

589 The authors declare that they have no competing interests exist.

590

591 **Author Contributions:**

592 Study conception and design: SRL, ZQW, JC and HS. Acquisition of data: MJ, HRZ,  
593 ZXL and JJW. Analysis and interpretation of data: SRL, MJ and HS. Drafting of  
594 manuscript: SRL, MJ and HRZ. Critical revision of manuscript: ZQW, JC and HS.  
595 All authors have read and agreed to the published version of the manuscript.

596

597 **References**

- 598 1. Neurath MF. Targeting immune cell circuits and trafficking in inflammatory bowel disease.  
599 *Nat Immunol.* 2019; 20(8): 970-9. doi: 10.1038/s41590-019-0415-0.
- 600 2. Long SR, Shang WX, Zhang HR, Jiang M, Wang JJ, Liu RD, et al. *Trichinella*-derived  
601 protein ameliorates colitis by altering the gut microbiome and improving intestinal barrier  
602 function. *Int Immunopharmacol.* 2024; 127: 111320. doi: 10.1016/j.intimp.2023.111320.
- 603 3. Windsor JW, Kaplan GG. Evolving epidemiology of IBD. *Curr Gastroenterol Rep.* 2019;  
604 21(8): 40. doi: 10.1007/s11894-019-0705-6.
- 605 4. Kaplan GG. The global burden of IBD: from 2015 to 2025. *Nat Rev Gastroenterol Hepatol.*  
606 2015; 12(12): 720-7. doi: 10.1038/nrgastro.2015.150.
- 607 5. Chu KM, Watermeyer G, Shelly L, Janssen J, May TD, Brink K, et al. Childhood helminth  
608 exposure is protective against inflammatory bowel disease: a case control study in South  
609 Africa. *Inflamm Bowel Dis.* 2013; 19(3): 614-20. doi: 10.1097/MIB.0b013e31827f27f4.
- 610 6. Bodammer P, Waitz G, Loebermann M, Holtfreter MC, Maletzki C, Krueger MR, et al.  
611 *Schistosoma mansoni* infection but not egg antigen promotes recovery from colitis in outbred  
612 NMRI mice. *Digestive diseases and sciences.* 2011; 56(1): 70-8. doi:  
613 10.1007/s10620-010-1237-y.
- 614 7. Hang L, Blum AM, Setiawan T, Urban JP, Jr., Stoyanoff KM, Weinstock JV.  
615 *Heligmosomoides polygyrus bakeri* infection activates colonic Foxp3+ T cells enhancing  
616 their capacity to prevent colitis. *J Immunol.* 2013; 191(4): 1927-34. doi:  
617 10.4049/jimmunol.1201457.
- 618 8. Cho MK, Park MK, Kang SA, Choi SH, Ahn SC, Yu HS. *Trichinella spiralis* infection  
619 suppressed gut inflammation with CD4(+)CD25(+)Foxp3(+) T cell recruitment. *Korean J  
620 Parasitol.* 2012; 50(4): 385-90. doi: 10.3347/kjp.2012.50.4.385.
- 621 9. Reyes JL, Fernando MR, Lopes F, Leung G, Mancini NL, Matisz CE, et al. IL-22 restrains  
622 tapeworm-mediated protection against experimental colitis via regulation of IL-25 expression.  
623 *PLoS Pathog.* 2016; 12(4): e1005481. doi: 10.1371/journal.ppat.1005481.
- 624 10. Manichanh C, Borruel N, Casellas F, Guarner F. The gut microbiota in IBD. *Nat Rev  
625 Gastroenterol Hepatol.* 2012; 9(10): 599-608. doi: 10.1038/nrgastro.2012.152.
- 626 11. Gensollen T, Iyer SS, Kasper DL, Blumberg RS. How colonization by microbiota in early  
627 life shapes the immune system. *Science.* 2016; 352(6285): 539-44. doi:  
628 10.1126/science.aad9378.
- 629 12. Shen ZH, Zhu CX, Quan YS, Yang ZY, Wu S, Luo WW, et al. Relationship between  
630 intestinal microbiota and ulcerative colitis: Mechanisms and clinical application of probiotics  
631 and fecal microbiota transplantation. *World J Gastroenterol.* 2018; 24(1): 5-14. doi:  
632 10.3748/wjg.v24.i1.5.
- 633 13. Zuo T, Kamm MA, Colombel JF, Ng SC. Urbanization and the gut microbiota in health and  
634 inflammatory bowel disease. *Nat Rev Gastroenterol Hepatol.* 2018; 15(7): 440-52. doi:  
635 10.1038/s41575-018-0003-z.
- 636 14. Varyani F, Fleming JO, Maizels RM. Helminths in the gastrointestinal tract as modulators of  
637 immunity and pathology. *Am J Physiol Gastrointest Liver Physiol.* 2017; 312(6): G537-g49.

doi: 10.1152/ajppg.00024.2017.

15. Long SR, Shang WX, Jiang M, Li JF, Liu RD, Wang ZQ, et al. Preexisting *Trichinella spiralis* infection attenuates the severity of *Pseudomonas aeruginosa*-induced pneumonia. PLoS Negl Trop Dis. 2022; 16(5): e0010395. doi: 10.1371/journal.pntd.0010395.

16. Ashour DS. *Trichinella spiralis* immunomodulation: an interactive multifactorial process. Expert Rev Clin Immunol. 2013; 9(7): 669-75. doi: 10.1586/1744666x.2013.811187.

17. Elmehy DA, Abdelhai DI, Elkholly RA, Elkholly MM, Tahoob DM, Elkholly RA, et al. Immunoprotective inference of experimental chronic *Trichinella spiralis* infection on house dust mites induced allergic airway remodeling. Acta Trop. 2021; 220: 105934. doi: 10.1016/j.actatropica.2021.105934.

18. Chu KB, Lee HA, Kang HJ, Moon EK, Quan FS. Preliminary *Trichinella spiralis* infection ameliorates subsequent RSV infection-induced inflammatory response. Cells. 2020; 9(5): 1314. doi: 10.3390/cells9051314.

19. Furze RC, Hussell T, Selkirk ME. Amelioration of influenza-induced pathology in mice by coinfection with *Trichinella spiralis*. Infect Immun. 2006; 74(3): 1924-32. doi: 10.1128/iai.74.3.1924-1932.2006.

20. Xue Y, Xu YF, Zhang B, Huang HB, Pan TX, Li JY, et al. *Trichinella spiralis* infection ameliorates the severity of *Citrobacter rodentium*-induced experimental colitis in mice. Exp Parasitol. 2022; 238: 108264. doi: 10.1016/j.exppara.2022.108264.

21. Ashour DS, Othman AA, Shareef MM, Gaballah HH, Mayah WW. Interactions between *Trichinella spiralis* infection and induced colitis in mice. J Helminthol. 2014; 88(2): 210-8. doi: 10.1017/s0022149x13000059.

22. Zhao Y, Liu MY, Wang XL, Liu XL, Yang Y, Zou HB, et al. Modulation of inflammatory bowel disease in a mouse model following infection with *Trichinella spiralis*. Vet Parasitol. 2013; 194(2-4): 211-6. doi: 10.1016/j.vetpar.2013.01.058.

23. Xu J, Yu P, Wu L, Liu M, Lu Y. Effect of *Trichinella spiralis* intervention on TNBS-induced experimental colitis in mice. Immunobiology. 2019; 224(1): 147-53. doi: 10.1016/j.imbio.2018.09.005.

24. Raygoza Garay JA, Turpin W, Lee SH, Smith MI, Goethel A, Griffiths AM, et al. Gut microbiome composition is associated with future onset of Crohn's disease in healthy first-degree relatives. Gastroenterology. 2023; 165(3): 670-81. doi: 10.1053/j.gastro.2023.05.032.

25. Schirmer M, Franzosa EA, Lloyd-Price J, McIver LJ, Schwager R, Poon TW, et al. Dynamics of metatranscription in the inflammatory bowel disease gut microbiome. Nat Microbiol. 2018; 3(3): 337-46. doi: 10.1038/s41564-017-0089-z.

26. Sun XM, Hao CY, Wu AQ, Luo ZN, El-Ashram S, Alouffii A, et al. *Trichinella spiralis* -induced immunomodulation signatures on gut microbiota and metabolic pathways in mice. PLoS Pathog. 2024; 20(1): e1011893. doi: 10.1371/journal.ppat.1011893.

27. Li C, Liu Y, Liu X, Bai X, Jin X, Xu F, et al. The gut microbiota contributes to changes in the host immune response induced by *Trichinella spiralis*. PLoS Negl Trop Dis. 2023; 17(8): e0011479. doi: 10.1371/journal.pntd.0011479.

28. Chen HL, Xing X, Zhang B, Huang HB, Shi CW, Yang GL, et al. Higher mucosal type II immunity is associated with increased gut microbiota diversity in BALB/c mice after *Trichinella spiralis* infection. Mol Immunol. 2021; 138: 87-98. doi:

682 10.1016/j.molimm.2021.07.014.

683 29. Pereira FC, Wasmund K, Cobankovic I, Jehmlich N, Herbold CW, Lee KS, et al. Rational  
684 design of a microbial consortium of mucosal sugar utilizers reduces *Clostridioides difficile*  
685 colonization. *Nature communications*. 2020; 11(1): 5104. doi: 10.1038/s41467-020-18928-1.

686 30. De A, Chen W, Li H, Wright JR, Lamendella R, Lukin DJ, et al. Bacterial swarmers enriched  
687 during intestinal stress ameliorate damage. *Gastroenterology*. 2021; 161(1): 211-24. doi:  
688 10.1053/j.gastro.2021.03.017.

689 31. Liu X, Zhang Y, Li W, Zhang B, Yin J, Liuqi S, et al. Fucoidan ameliorated dextran sulfate  
690 sodium-induced ulcerative colitis by modulating gut microbiota and bile acid metabolism. *J  
691 Agric Food Chem*. 2022; 70(47): 14864-76. doi: 10.1021/acs.jafc.2c06417.

692 32. Huang Y, Yang Q, Mi X, Qiu L, Tao X, Zhang Z, et al. Ripened Pu-erh tea extract promotes  
693 gut microbiota resilience against dextran sulfate sodium induced colitis. *J Agric Food Chem*.  
694 2021; 69(7): 2190-203. doi: 10.1021/acs.jafc.0c07537.

695 33. Zhou F, Mai T, Wang Z, Zeng Z, Shi J, Zhang F, et al. The improvement of intestinal  
696 dysbiosis and hepatic metabolic dysfunction in dextran sulfate sodium-induced colitis mice:  
697 effects of curcumin. *Journal of gastroenterology and hepatology*. 2023; 38(8): 1333-45. doi:  
698 10.1111/jgh.16205.

699 34. Sun M, Wu W, Liu Z, Cong Y. Microbiota metabolite short chain fatty acids, GPCR, and  
700 inflammatory bowel diseases. *J Gastroenterol*. 2017; 52(1): 1-8. doi:  
701 10.1007/s00535-016-1242-9.

702 35. Guo C, Wang Y, Zhang S, Zhang X, Du Z, Li M, et al. *Crataegus pinnatifida* polysaccharide  
703 alleviates colitis via modulation of gut microbiota and SCFAs metabolism. *Int J Biol  
704 Macromol*. 2021; 181: 357-68. doi: 10.1016/j.ijbiomac.2021.03.137.

705 36. Zhou C, Li L, Li T, Sun L, Yin J, Guan H, et al. SCFAs induce autophagy in intestinal  
706 epithelial cells and relieve colitis by stabilizing HIF-1 $\alpha$ . *J Mol Med (Berl)*. 2020; 98(8):  
707 1189-202. doi: 10.1007/s00109-020-01947-2.

708 37. He P, Zhang Y, Chen R, Tong Z, Zhang M, Wu H. The maca protein ameliorates  
709 DSS-induced colitis in mice by modulating the gut microbiota and production of SCFAs.  
710 *Food Funct*. 2023; 14(23): 10329-46. doi: 10.1039/d3fo03654e.

711 38. Vinolo MA, Rodrigues HG, Nachbar RT, Curi R. Regulation of inflammation by short chain  
712 fatty acids. *Nutrients*. 2011; 3(10): 858-76. doi: 10.3390/nu3100858.

713 39. Duscha A, Gisevius B, Hirschberg S, Yissachar N, Stangl GI, Dawin E, et al. Propionic acid  
714 shapes the multiple sclerosis disease course by an immunomodulatory mechanism. *Cell*. 2020;  
715 180(6): 1067-80.e16. doi: 10.1016/j.cell.2020.02.035.

716 40. Wang X, Cai Z, Wang Q, Wu C, Sun Y, Wang Z, et al. *Bacteroides methylmalonyl-CoA*  
717 mutase produces propionate that promotes intestinal goblet cell differentiation and  
718 homeostasis. *Cell Host Microbe*. 2024; 32(1): 63-78.e7. doi: 10.1016/j.chom.2023.11.005.

719 41. Moore KW, de Waal Malefyt R, Coffman RL, O'Garra A. Interleukin-10 and the  
720 interleukin-10 receptor. *Annu Rev Immunol*. 2001; 19: 683-765. doi:  
721 10.1146/annurev.immunol.19.1.683.

722 42. Gustafsson JK, Johansson MEV. The role of goblet cells and mucus in intestinal homeostasis.  
723 *Nat Rev Gastroenterol Hepatol*. 2022; 19(12): 785-803. doi: 10.1038/s41575-022-00675-x.

724 43. Long SR, Wang ZQ, Liu RD, Liu LN, Li LG, Jiang P, et al. Molecular identification of  
725 *Trichinella spiralis* nudix hydrolase and its induced protective immunity against trichinellosis

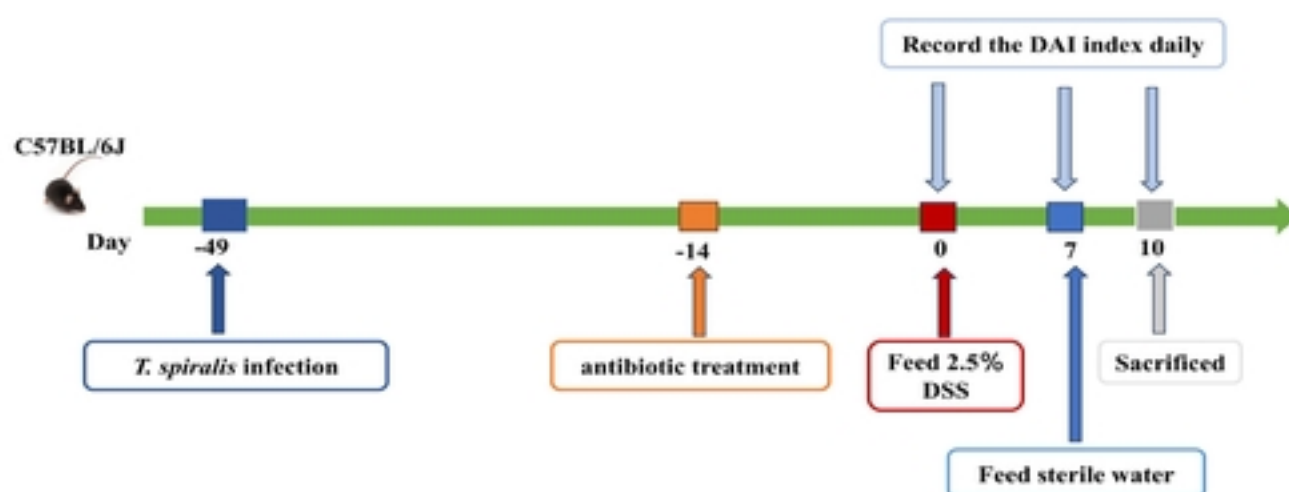
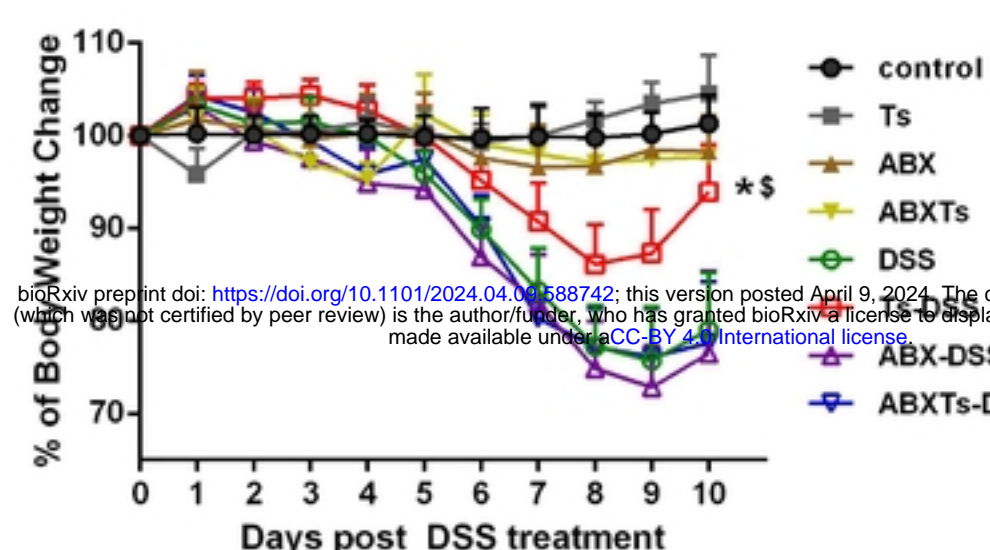
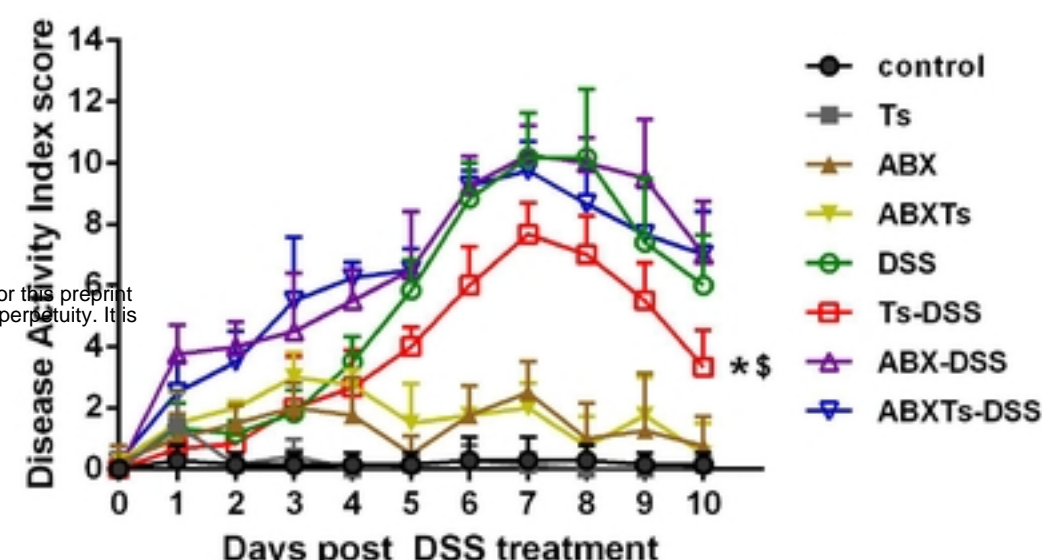
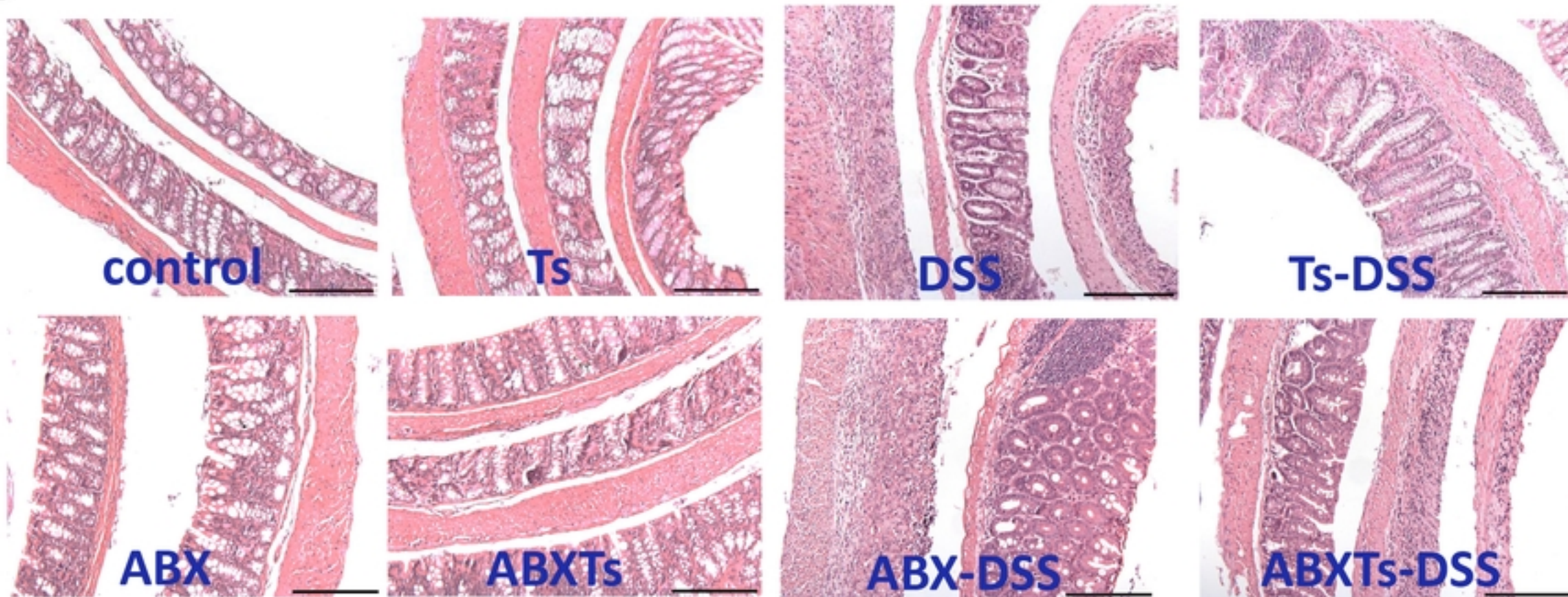
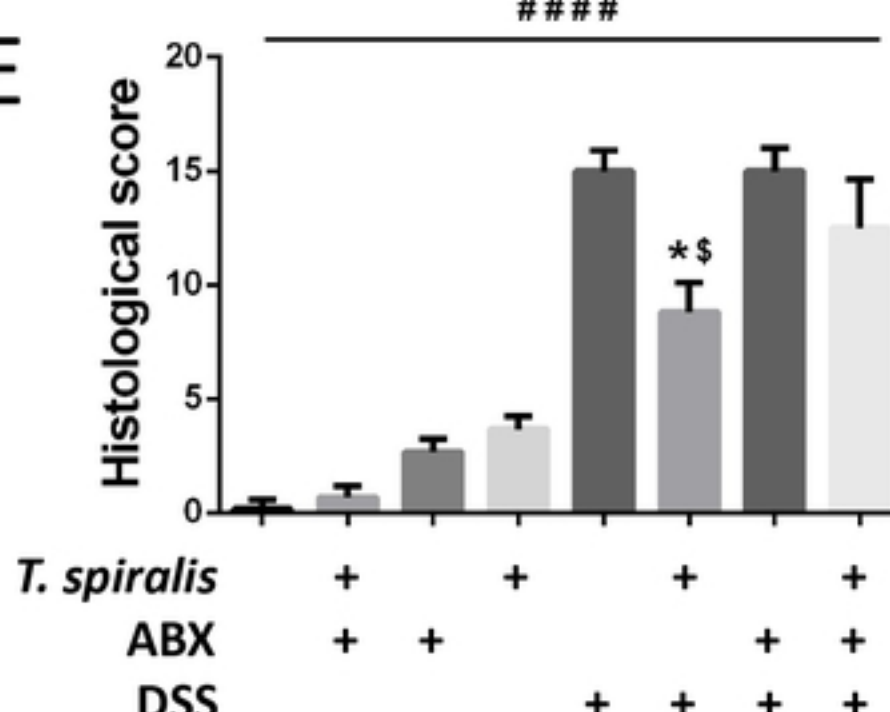
726 in BALB/c mice. *Parasit Vectors*. 2014; 7: 600. doi: 10.1186/s13071-014-0600-9.

727 44. Long SR, Liu RD, Kumar DV, Wang ZQ, Su CW. Immune protection of a helminth protein  
728 inInduced colitis model in mice. *Front Immunol*. 2021; 12: 664998. doi: 10 the  
729 DSS-.3389/fimmu.2021.664998.

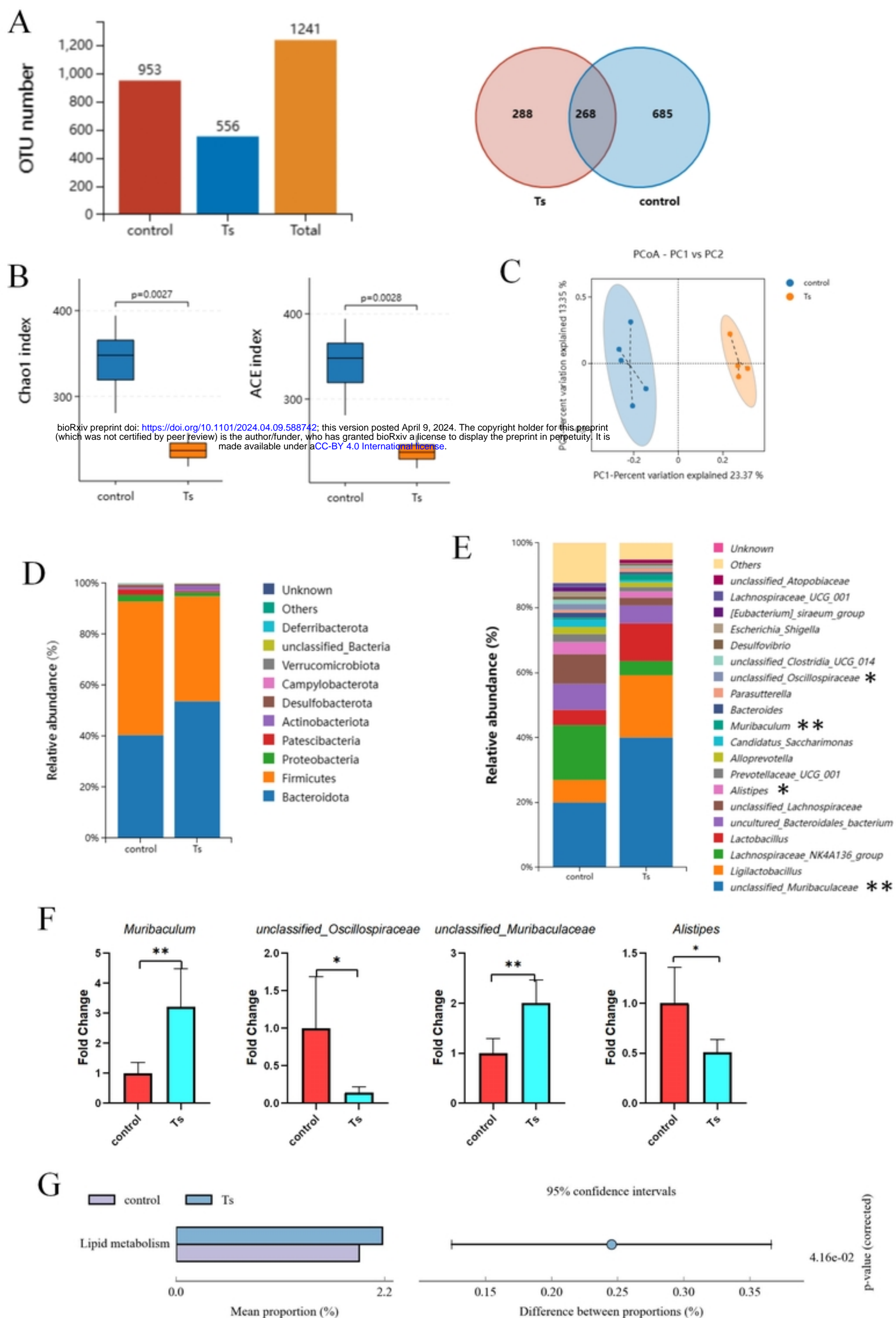
730 45. Wang L, Xie H, Xu L, Liao Q, Wan S, Yu Z, et al. rSj16 protects against DSS-induced colitis  
731 by inhibiting the PPAR- $\alpha$  signaling pathway. *Theranostics*. 2017; 7(14): 3446-60. doi:  
732 10.7150/thno.20359.

733 46. Chong J, Xia J. MetaboAnalystR: an R package for flexible and reproducible analysis of  
734 metabolomics data. *Bioinformatics*. 2018; 34(24): 4313-4. doi:  
735 10.1093/bioinformatics/bty528.

736

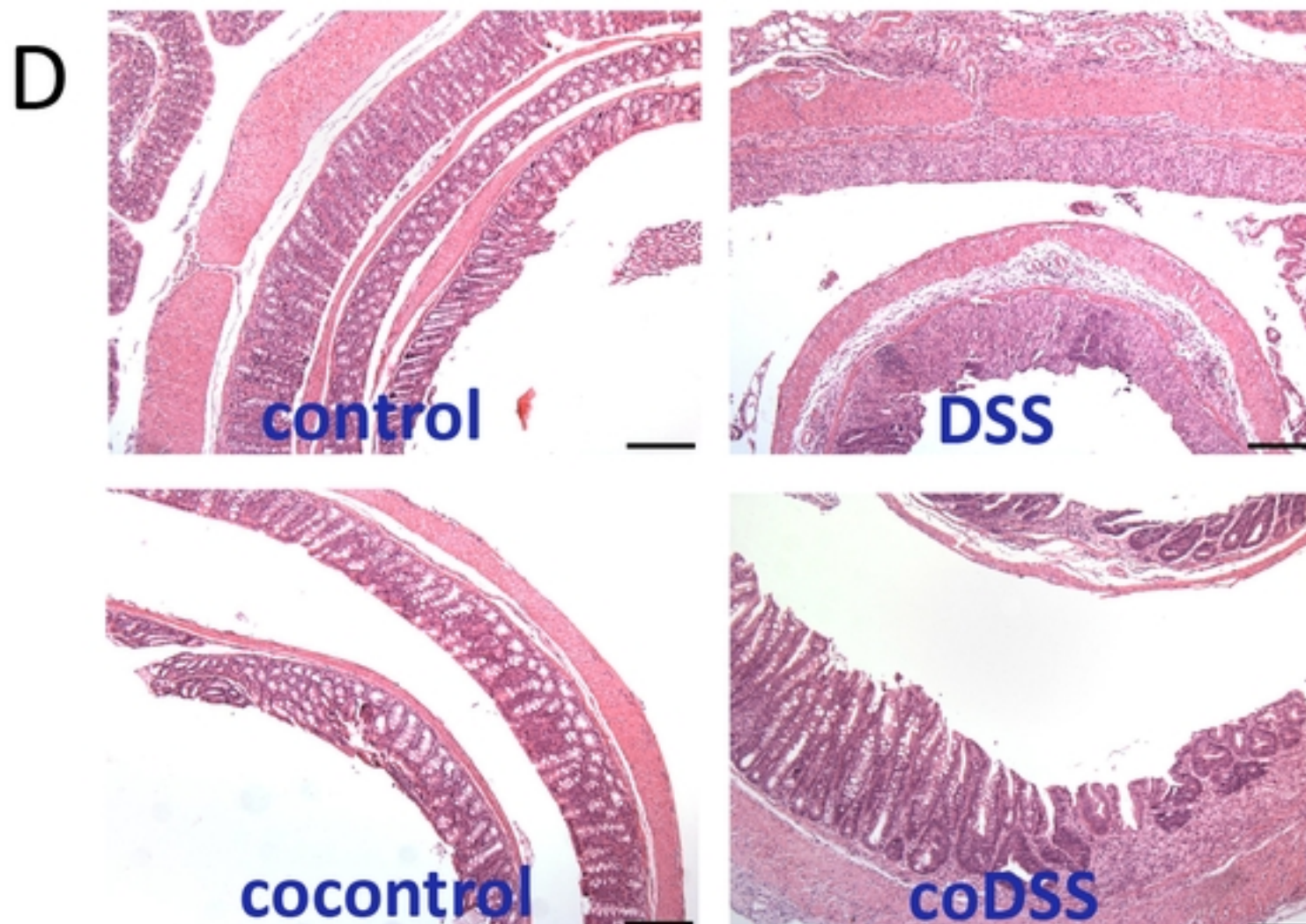
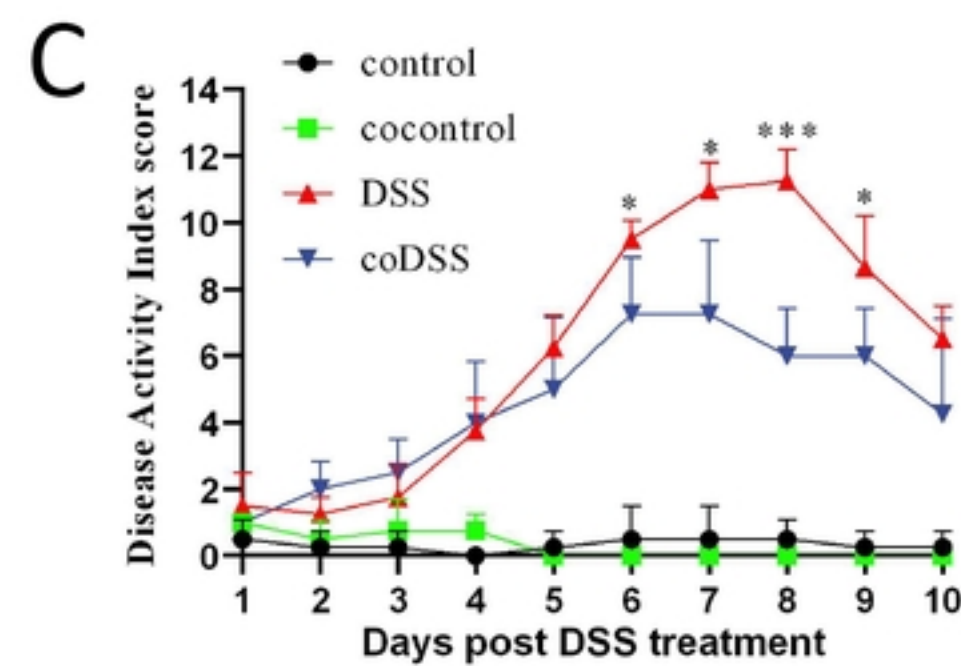
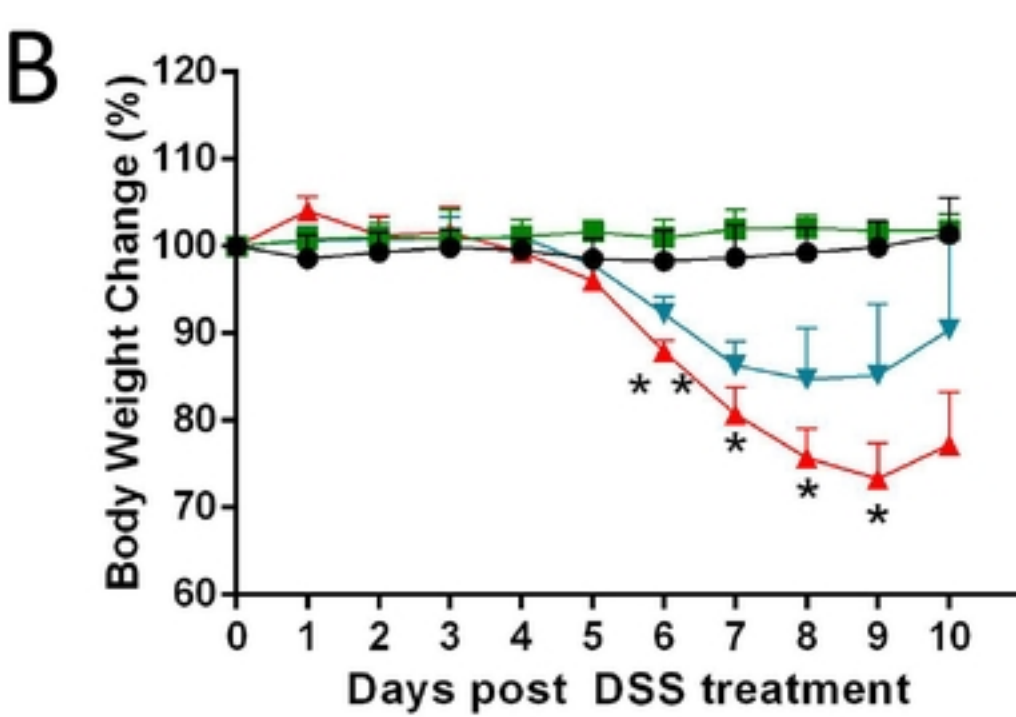
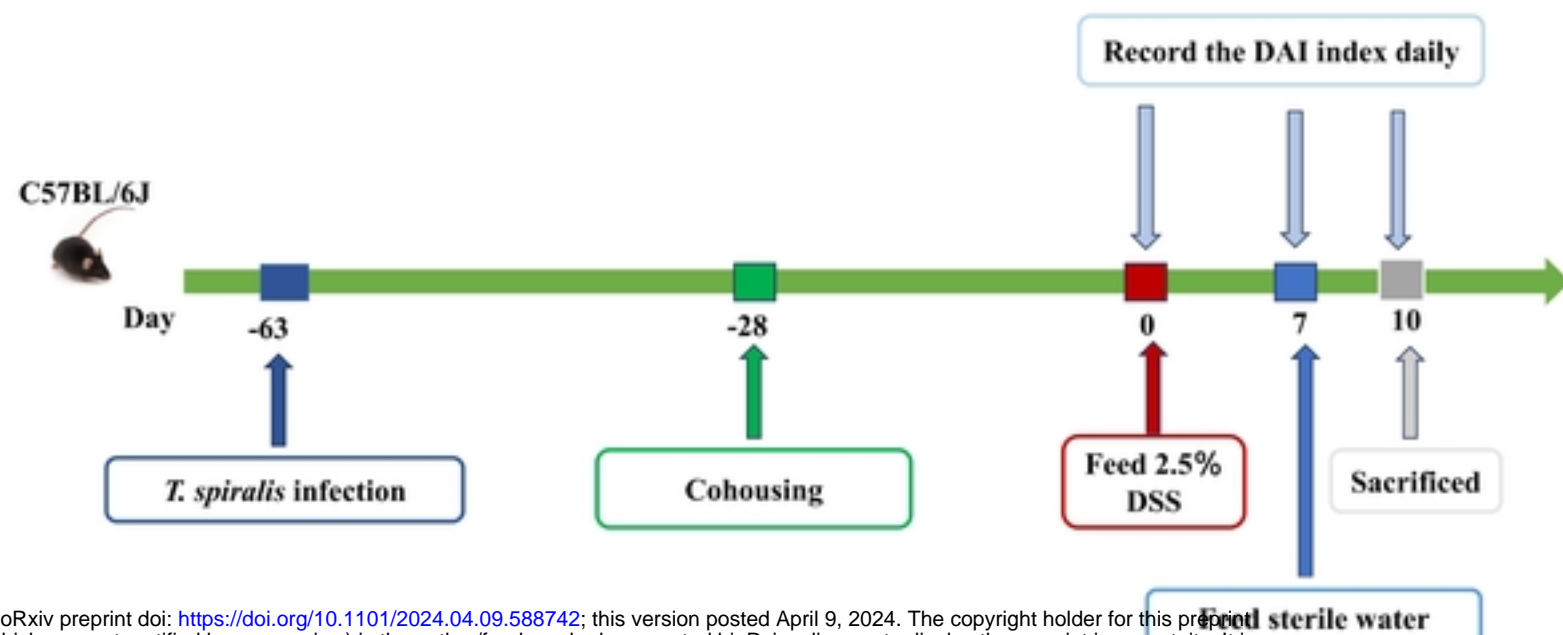
**Fig 1****B****C****D****E****Fig 1**

# Fig 2



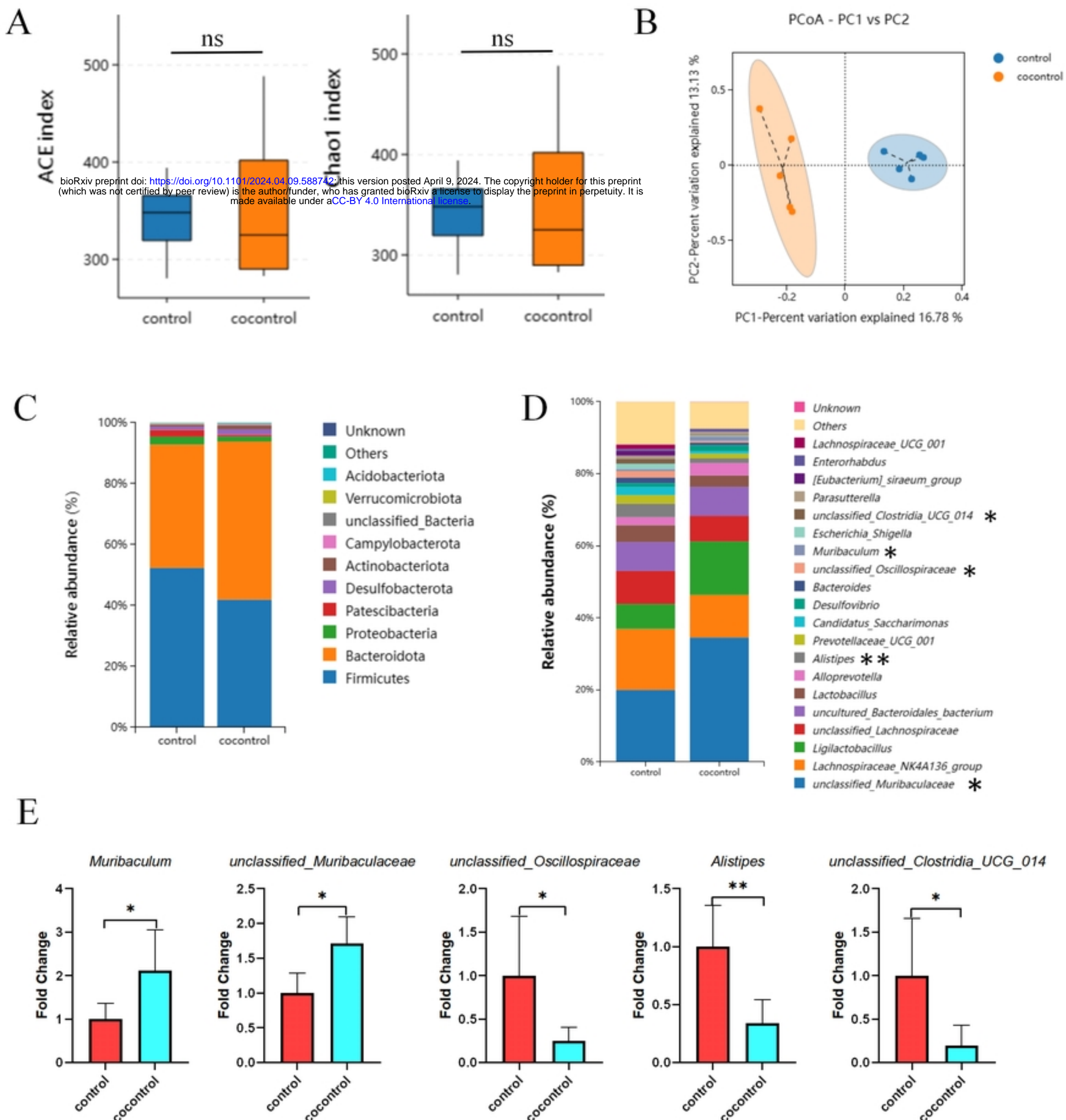
# Fig 2

# Fig 3

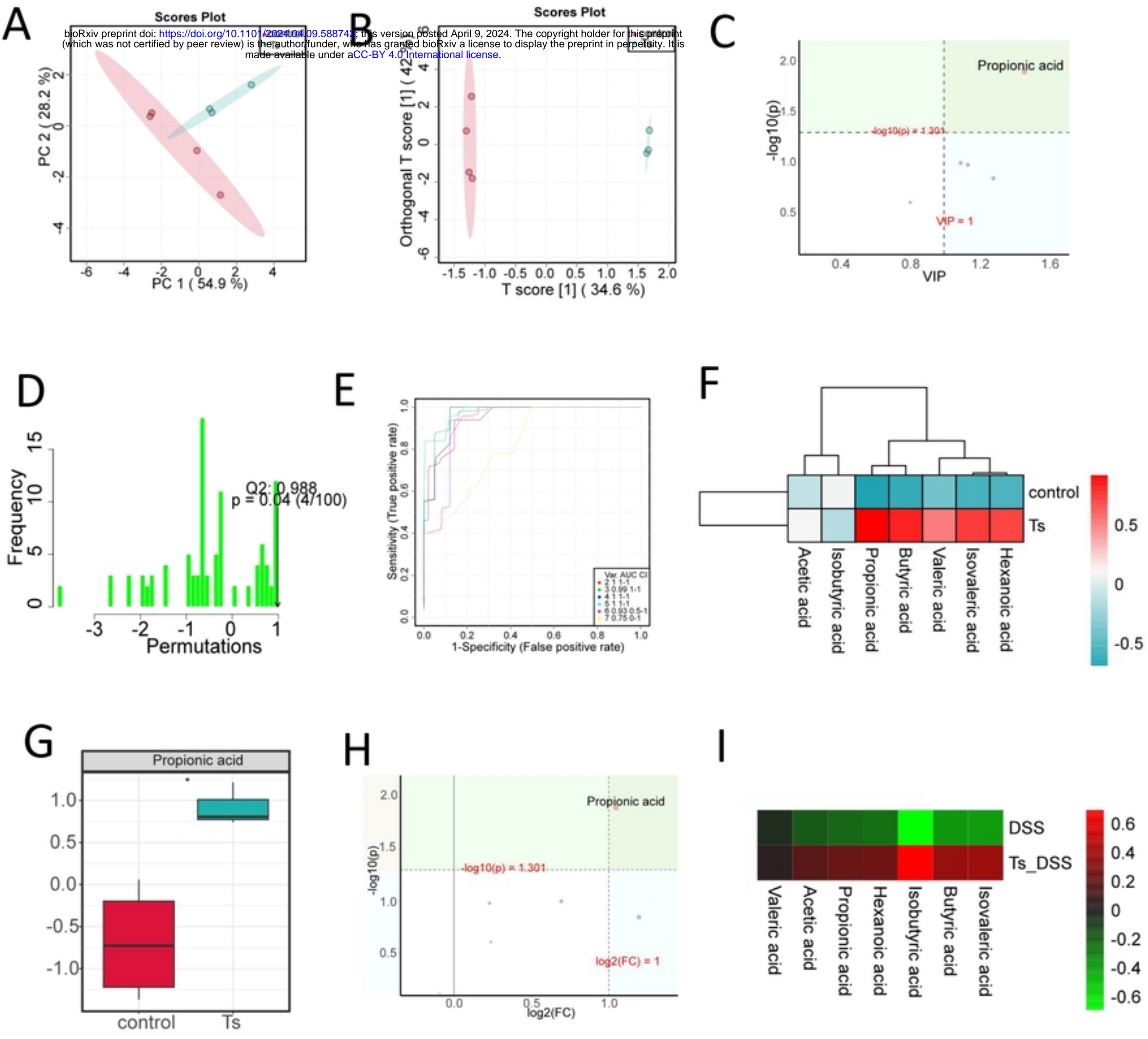


# Fig 3

# Fig 4

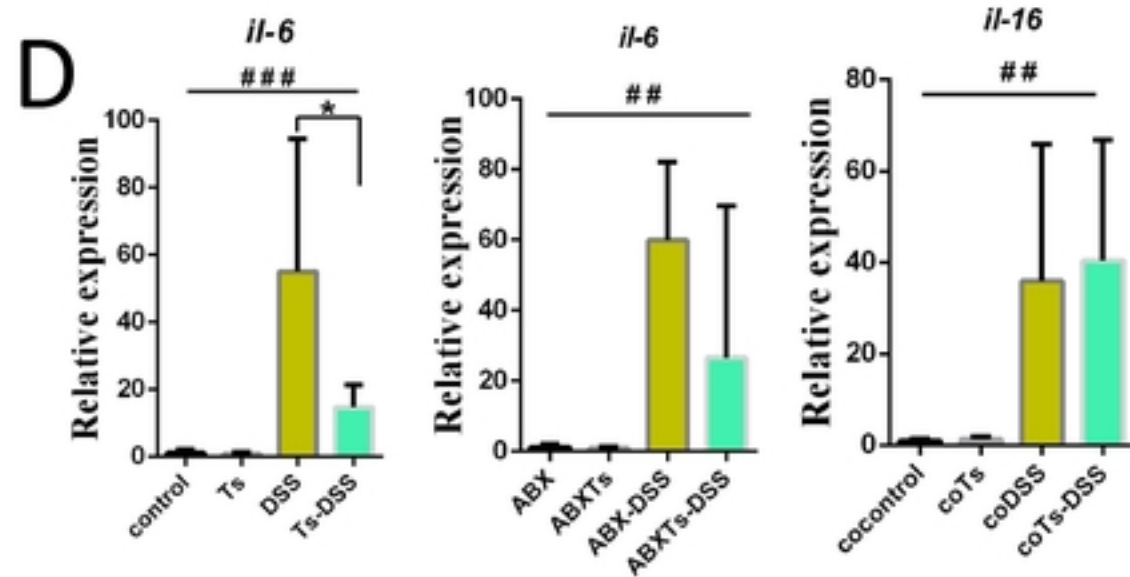
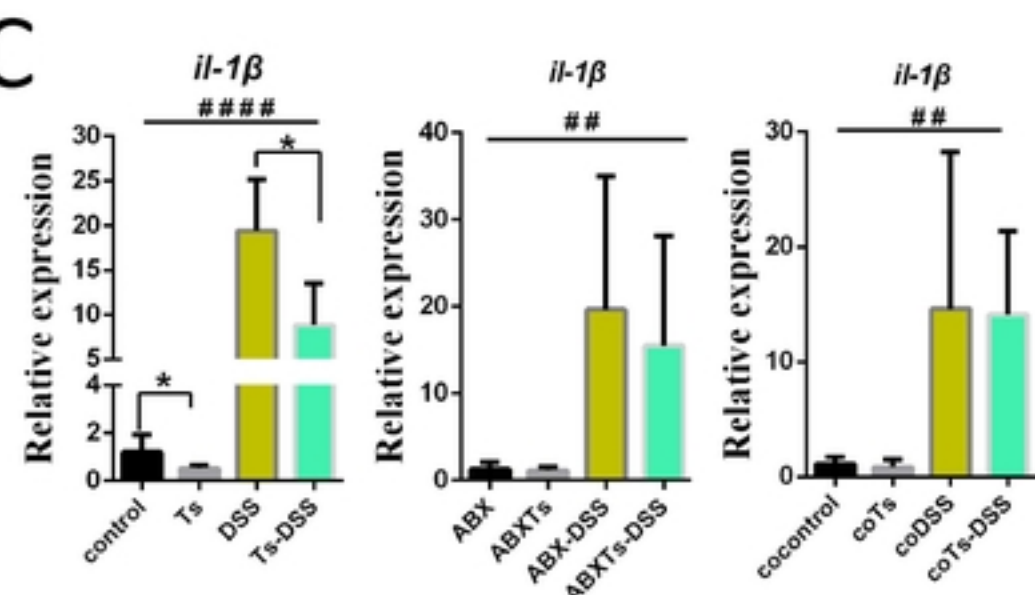
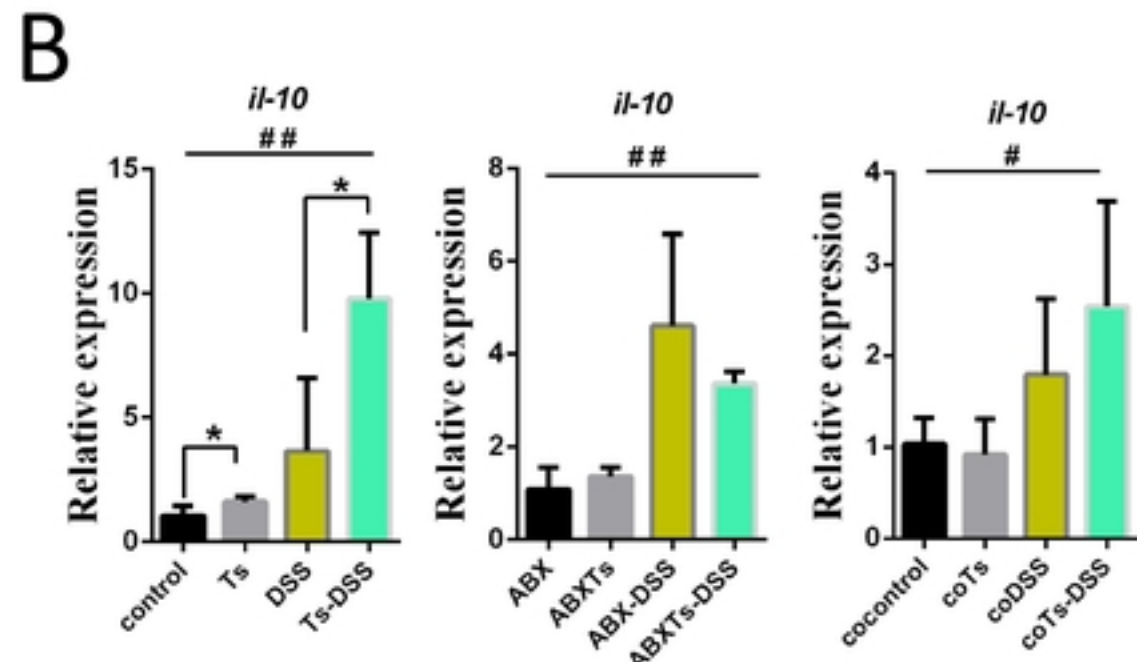
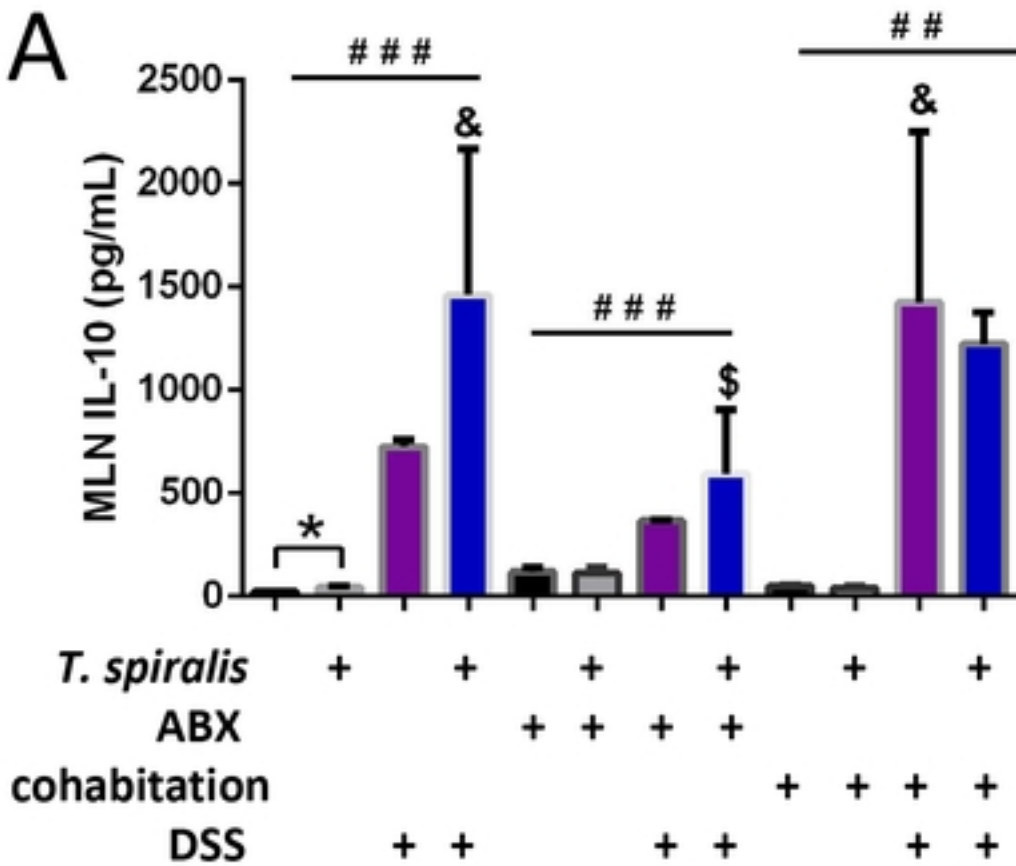


# Fig 4

**Fig 5****Fig 5**

# Fig 6

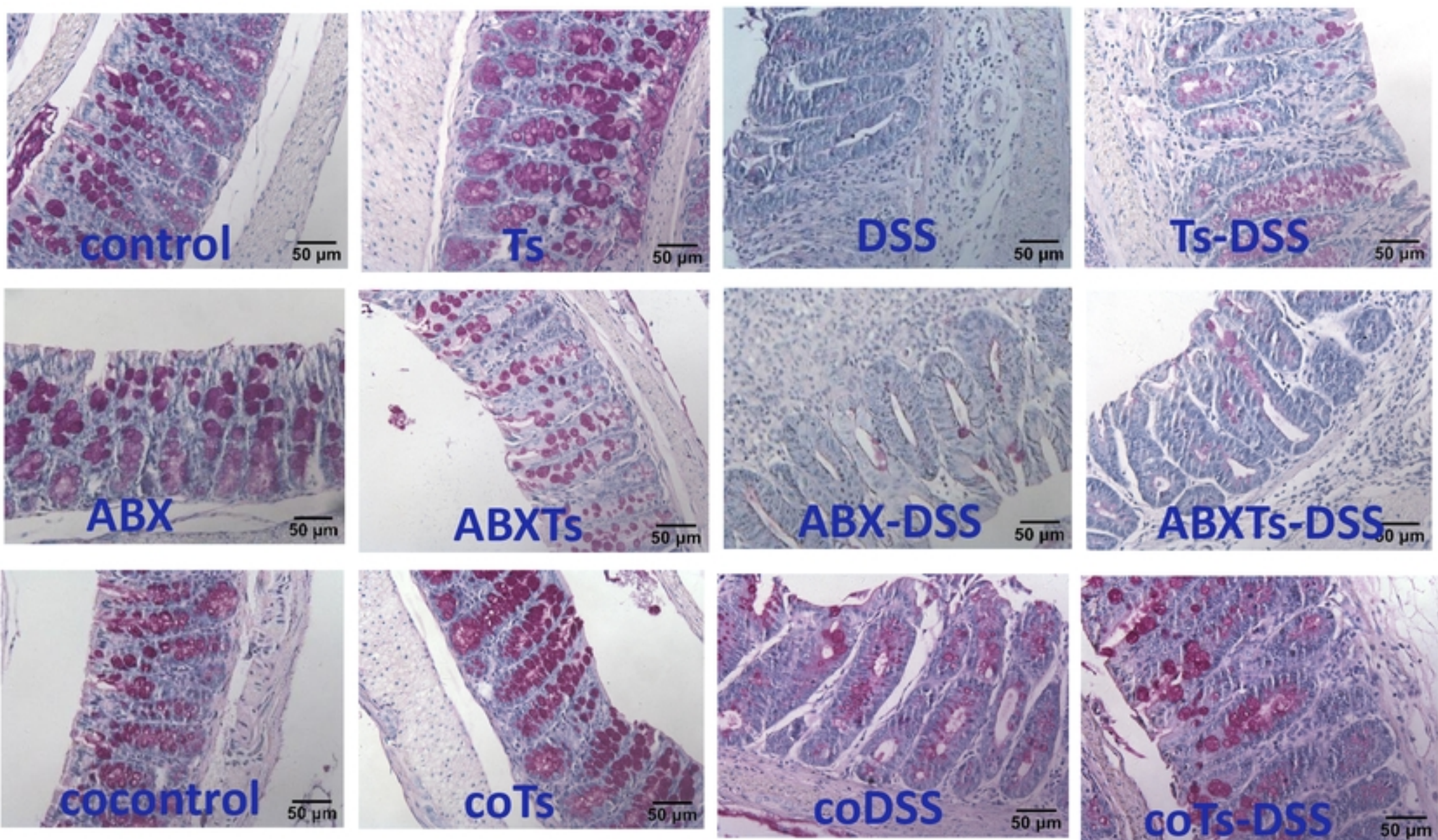
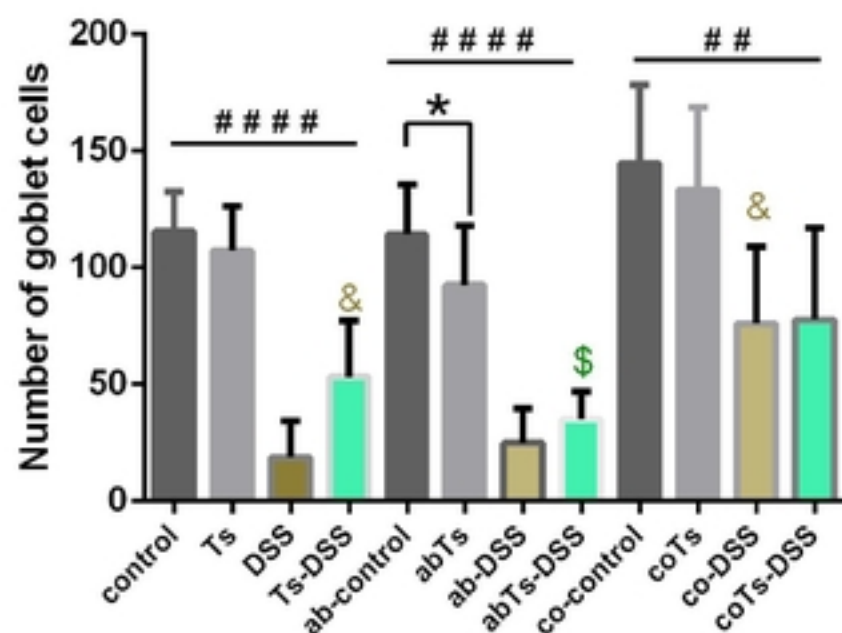
## MLN IL-10 production



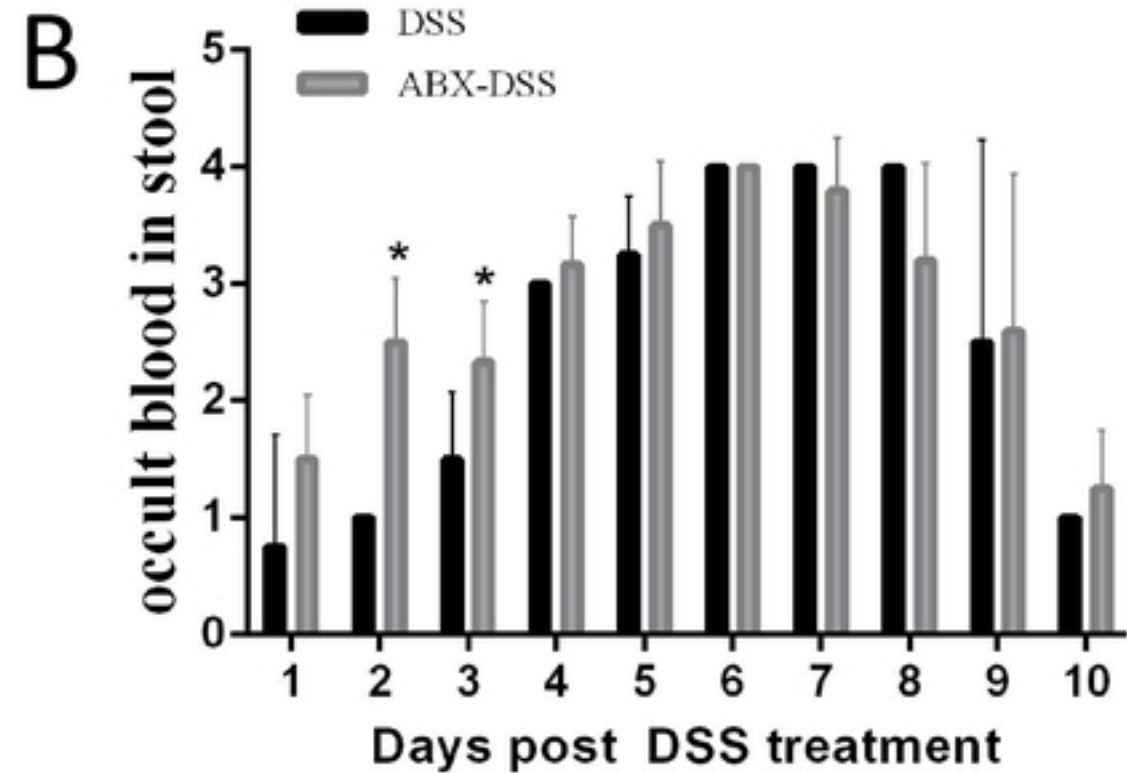
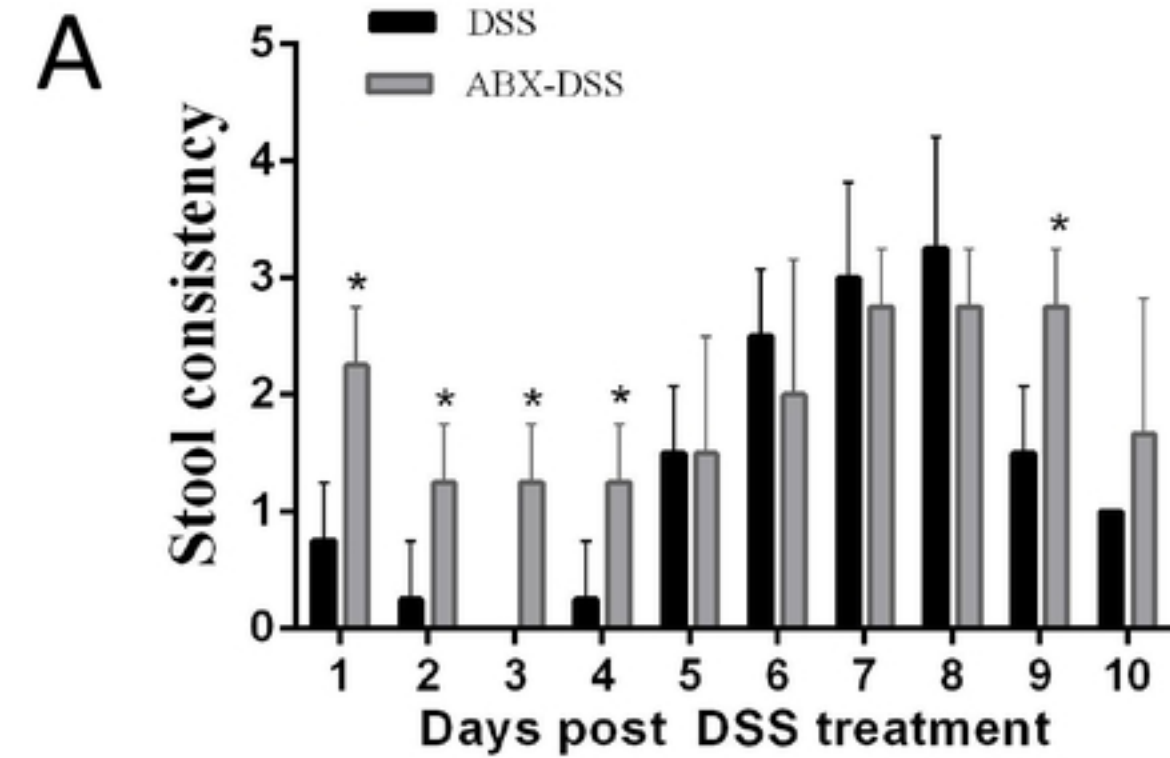
# Fig 6

**Fig 7**

bioRxiv preprint doi: <https://doi.org/10.1101/2024.04.09.588742>; this version posted April 9, 2024. The copyright holder for this preprint (which was not certified by peer review) is the author/funder, who has granted bioRxiv a license to display the preprint in perpetuity. It is made available under aCC-BY 4.0 International license.

**A****B****Fig 7**

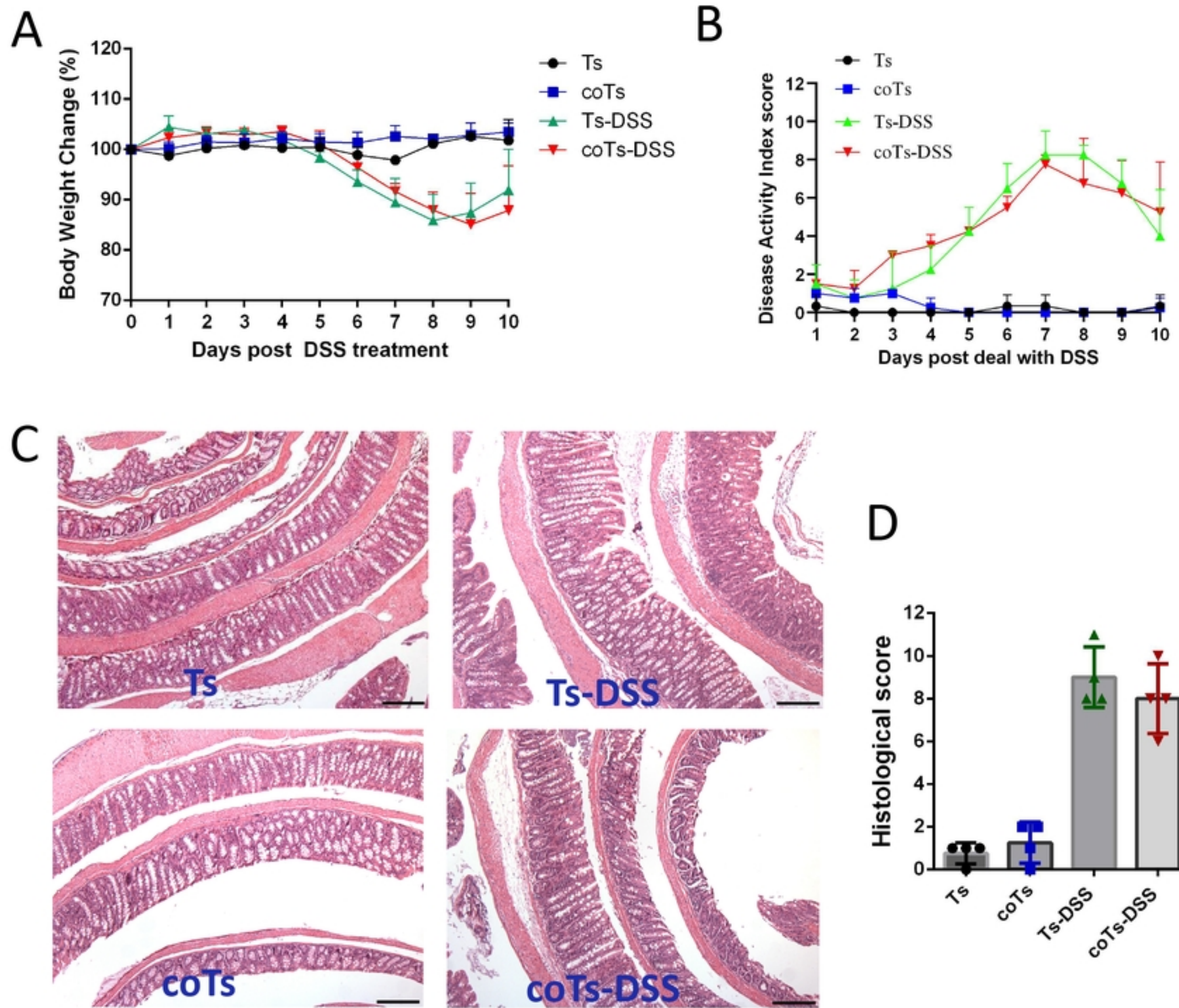
# S1 Fig



# S1 Fig

## S2 Fig

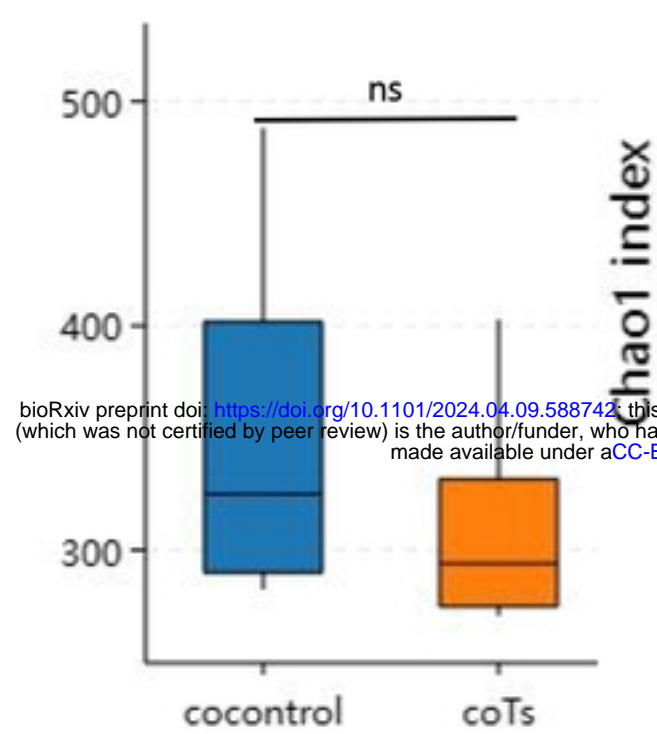
bioRxiv preprint doi: <https://doi.org/10.1101/2024.04.09.588742>; this version posted April 9, 2024. The copyright holder for this preprint (which was not certified by peer review) is the author/funder, who has granted bioRxiv a license to display the preprint in perpetuity. It is made available under aCC-BY 4.0 International license.



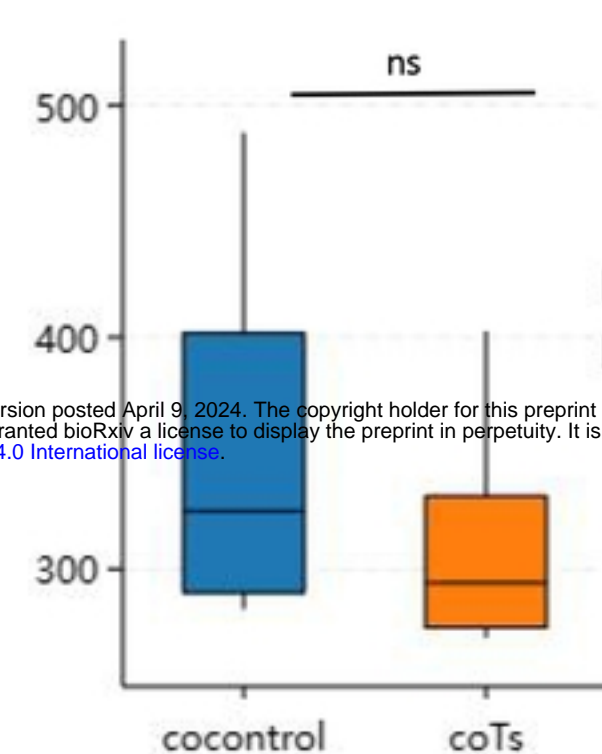
S2 Fig

# S3 Fig

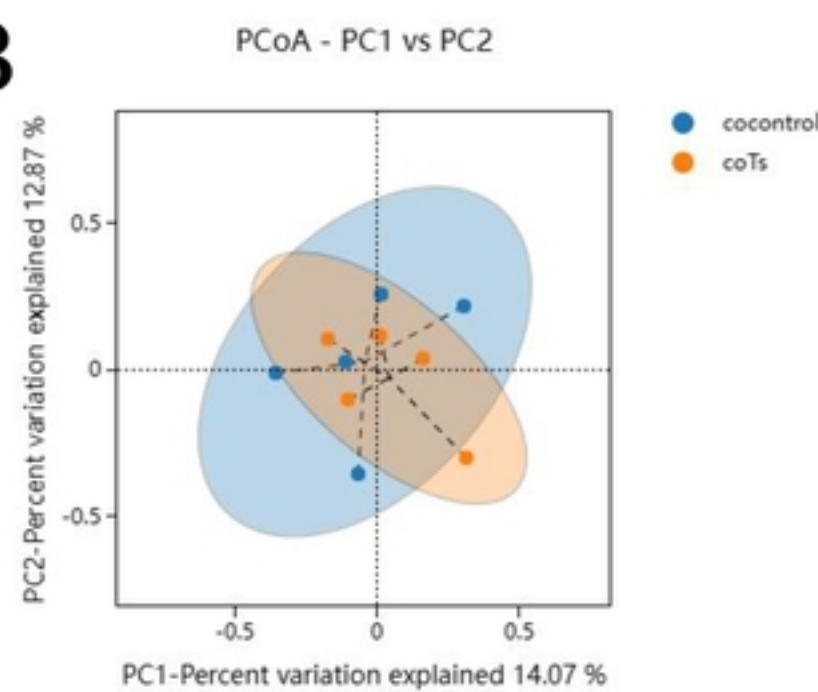
A



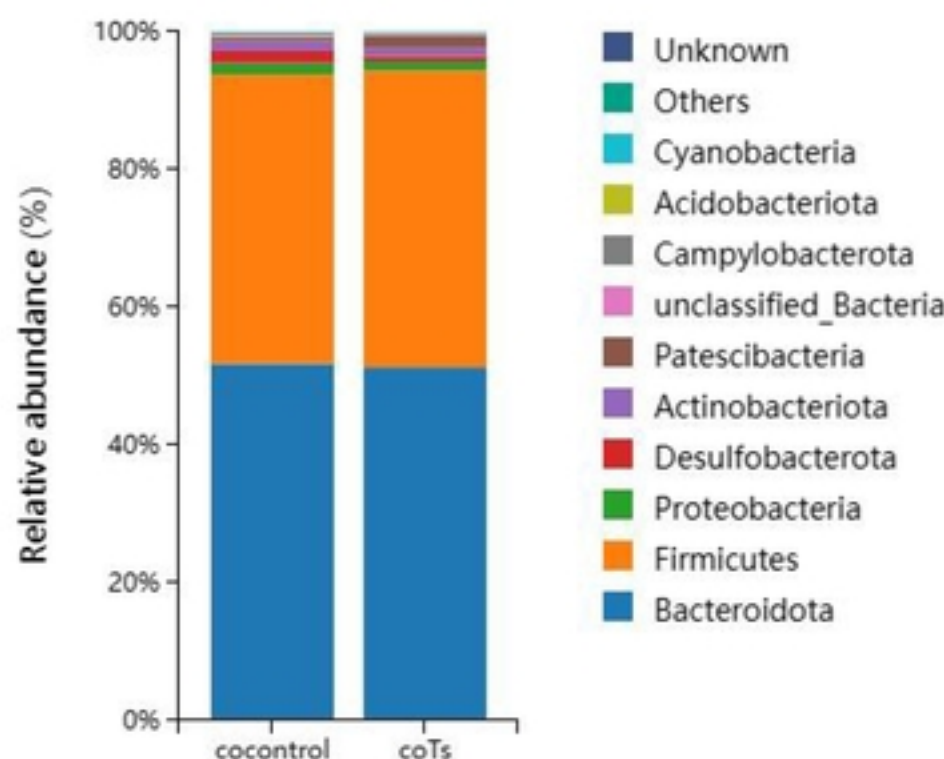
Chao1 index



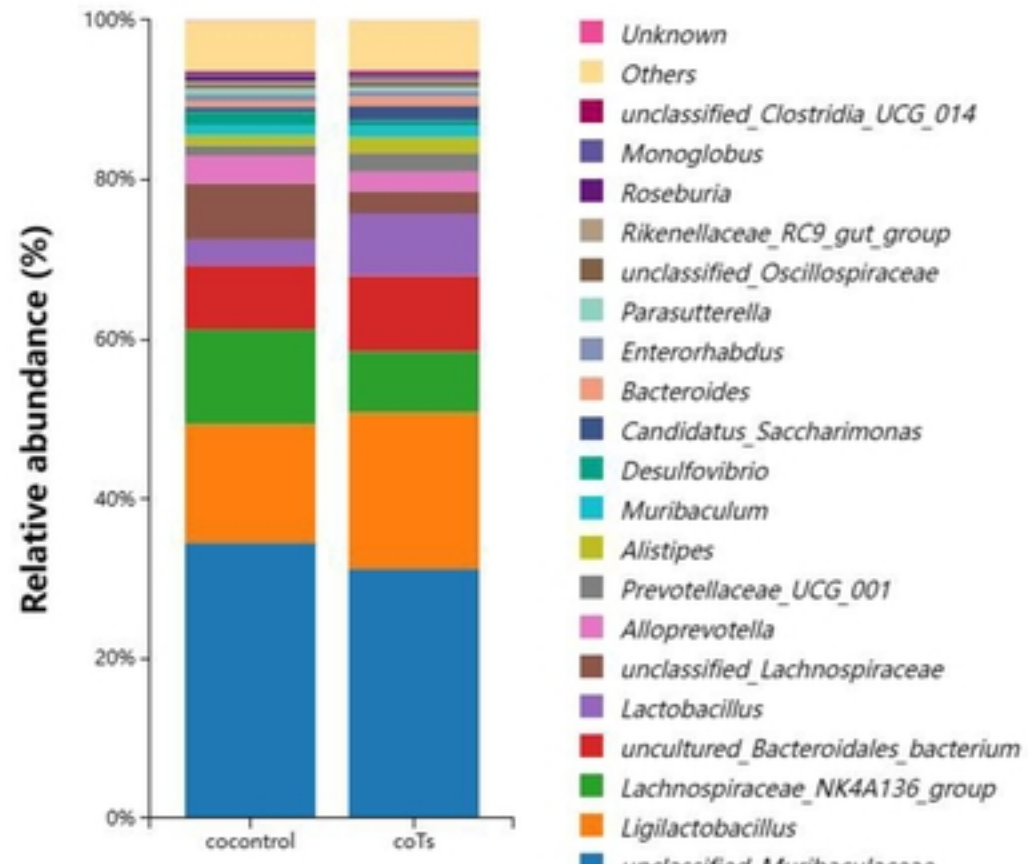
B



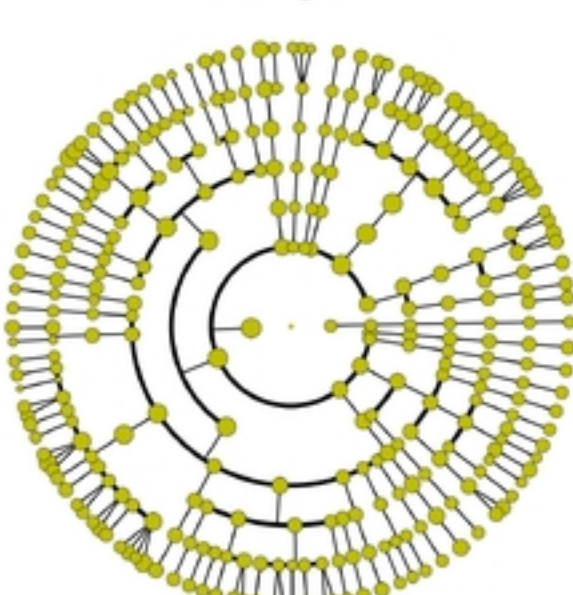
C



D



E



S3 Fig